

**NATIONAAL LUCHT- EN RUIMTEVAARTLABORATORIUM**  
**NATIONAL AEROSPACE LABORATORY NLR**  
**THE NETHERLANDS**

TECHNISCHE HOOGESCHOOL DELFT  
LUCHTVAART- EN RUIMTEVAARTTECHNIEK  
BIBLIOTHEEK  
Kluyverweg 1 - DELFT

7 DEC. 1976

NLR TR 75114 U

**TENSILE FAILURE OF UNIDIRECTIONAL COMPOSITE MATERIALS**

BY

W.G.J. 't HART, F.A. JACOBS and J.H. NASSETTE

TECHNISCHE UNIVERSITEIT DELFT  
LUCHTVAART- EN RUIMTEVAARTTECHNIEK  
BIBLIOTHEEK  
Kluyverweg 1 - 2629 HS DELFT



Reprints from this publication may be made on condition that full credit be given to the Nationaal Lucht- en Ruimtevaartlaboratorium (National Aerospace Laboratory NLR) and the Author(s)

## DOCUMENT CONTROL SHEET

	ORIGINATOR'S REF. NLR TR 75114 U		SECURITY CLASS. Unclassified
ORIGINATOR	National Aerospace Laboratory NLR Amsterdam. The Netherlands		
TITLE	Tensile failure of unidirectional composite materials		
PRESENTED AT			
AUTHORS	W.G.J. 't Hart, F.A. Jacobs and J.H. Nassette	DATE 16-VII-'75	PP      ref 36      29
DESCRIPTORS	composite materials reinforcing fibres carbon fibres boron fibres glass fibres epoxy resins reinforced plastics tensile strength	statistical distribution failure modes failure analysis crack propagation stress concentration	
ABSTRACT	<p>Theoretical strength predictions for unidirectional composite materials under tensile loading have been considered. Tensile tests on carbon/epoxy and boron/epoxy specimens were performed in order to compare the experimental strength data with the theoretical strength predictions, based on fibre strength distributions. It was concluded that for the tested carbon/epoxy specimens, the best fit was attained by the rule of mixtures. For boron/epoxy specimens, the bundle strength theory gave the best approximation.</p> <p>The use of the more refined strength predictions is not recommended as long as composites are fabricated with voids and non-uniformly distributed fibres.</p>		

NLR TR 75114 U

TENSILE FAILURE OF UNIDIRECTIONAL COMPOSITE MATERIALS

by

W.G.J. 't Hart, F.A. Jacobs and J.H. Nassette

SUMMARY


Theoretical strength predictions for unidirectional composite materials under tensile loading have been considered. Tensile tests on carbon/epoxy and boron/epoxy specimens were performed in order to compare the experimental strength data with the theoretical strength predictions, based on fibre strength distributions. It was concluded that for the tested carbon/epoxy specimens, the best fit was attained by the rule of mixtures. For boron/epoxy specimens, the bundle strength theory gave the best approximation.

The use of the more refined strength predictions is not recommended as long as composites are fabricated with voids and non-uniformly distributed fibres.

This investigation has been performed under contract with the Netherlands Agency for Aerospace Programs, NIVR.

Division: Structures and Materials

Prepared: WGJ'tH/ wsl

Approved: HPvL/ 

Completed : 16-VII-1975

NIVR Contractnumber: 1744

Ordernumber : 101.323

Typ. : GD

CONTENTS		Page
LIST OF SYMBOLS		3
1 INTRODUCTION		5
2 ANALYSIS OF THE TENSILE FAILURE MODES OF COMPOSITE MATERIALS		6
2.1 Introduction		6
2.2 Fibre strength distribution		6
2.3 Bundle strength		9
2.4 Strength prediction of composites, based on fibre strength distribution		11
2.5 Summary of strength predictions according to the discussed failure modes		20
3 EXPERIMENTAL RESULTS		21
3.1 Mechanical properties of fibres		21
3.2 Mechanical properties of bundles		23
3.3 Laminate tests		24
3.3.1 Carbon/epoxy specimens		24
3.3.1.1 Comparison of strength data with theoretical strength predictions		26
3.3.2 Boron/epoxy specimens		27
3.3.2.1 Comparison of strength data with theoretical strength predictions		28
4 CONSEQUENCES OF SCATTER IN COMPOSITE STRENGTH FOR DESIGN VALUES		28
5 DISCUSSION		30
6 CONCLUSIONS		32
7 REFERENCES		33
APPENDIX LOAD CONCENTRATION FACTOR (1 page)		
8 tables		
30 figures		

## LIST OF SYMBOLS

$A, B$	Statistical events
$A \cup B$	The union of the events A and B
$A \cap B$	The intersection of the events A and B
$E(\sigma^k)$	k-th moment of the random variable $\sigma$ of a distribution
$E_f$	Fibre modulus
$E_c$	Composite modulus
$E_m$	Matrix modulus
$F_a$	Design allowable strength
$F_{av}$	Mean value of a number of test data
$G_m$	Shear modulus of matrix
$f(\sigma)$	Probability density function of fibre strength
$g(\sigma)$	" " " of fibre segment strength
$p(\sigma)$	" " " of weakest fibre strength
$\omega(\sigma)$	" " " of layer strength
$F(\sigma)$	Cumulative distribution function of fibre strength
$G(\sigma)$	" " " of fibre segment strength
$P(\sigma)$	" " " of weakest fibre strength
$\Omega(\sigma)$	" " " of layer strength
$E_i$	Expected number of groups consisting of i broken fibres
$P_i$	Probability of at least i broken fibres in the composite
$K_i$	Load concentration factor associated with i broken fibres
$L$	Fibre length
$n$	Number of axial layers
$N$	Number of fibres
$V_f$	Fibre volume fraction
$s$	Standard deviation
$cv$	Coefficient of variation
$k$	One sided tolerance factor for the normal distribution
$var$	Variance
$\alpha$	Scale parameter of the Weibull distribution
$\beta$	Shape parameter of the Weibull distribution
$\delta$	Ineffective length
$\sigma$	Fibre strength

$\bar{\sigma}_f$	Mean fracture stress of a population of fibres
$\sigma_{ma}$	Matrix strength
$\sigma'_{ma}$	Stress in the matrix when the fibres fail
$\sigma_m$	Maximum fibre stress in a bundle of fibres
$\bar{\sigma}_B$	Mean fibre stress at bundle failure
$\sigma_{comp}$	Composite strength
$\sigma_{cb}$	The most probable value of the smallest strength in a sample of size n
$\sigma_{cum}$	Fibre stress at failure according to the cumulative failure mode
$\lambda(\sigma_{cb})$	Probability density function for the strength of the weakest layer in the cumulative weakening model
$\mu$	Mean of a distribution
$\psi_B$	Standard deviation of average fibre stress at bundle failure
$\phi$	A specified fraction of the fibre stress

## 1 INTRODUCTION

Composite materials containing strong and stiff continuous filaments are attractive for structural applications where high stiffness to weight and ultimate strength to weight are required. The advantage of composite materials is the possibility to create a structural material by adapting the fibre orientation to the stress condition. There are already some applications of composites in airplane design (Refs. 1 to 5), but the design criteria for most applications up to now are based on stiffness rather than strength.

For ample applications of composites in aircraft design, an understanding of the fracture behaviour under tensile and compressive loading is needed. A considerable amount of effort has been spent up to now to develop reliable strength criteria and to relate the composite properties to the mechanical properties of the constituent components. The development of strength criteria and their verification is often obstructed by the influence of production parameters that makes it difficult to produce a composite with constant properties. The first developed strength criteria take no account of the matrix properties since the matrix strength properties are small as compared to the fibre strength properties. However, it soon became evident that composite strength could not always be predicted by means of the mean strength of the reinforcing fibres. Later on the effect of the matrix properties on the failure mode was recognized and this has resulted in a more realistic approach of the composite strength problem. Today the general opinion is that the prediction of fracture strength of composite materials usually will be a statistical problem.

It is important to understand the failure mechanism of u.d. composites under uniaxial loading in the first place. For more complex loading conditions, failure criteria for orthotropic materials in plane stress condition have been developed, which can be presented in the three-dimensional  $\sigma_x - \sigma_y - \sigma_{xy}$  stress space by an ellipsoidal "failure surface". The intercepts of the failure surface with the co-ordinate axes in the stress space are the principal strengths, i.e., the uniaxial tensile and compressive strength and the pure shear strength. These principal strengths have to be determined by simple tests.



So it is evident that an understanding of the failure modes under tensile, compressive and shear loading is essential prior to the verification of the failure criteria under multiaxial loading.

In the present report the existing failure criteria for unidirectional composites under tensile load are discussed. In order to verify the discussed models, concerning uniaxial tensile strength, tensile tests have been carried out on carbon/epoxy and boron/epoxy composites. Prior to that the fibre properties have been determined by single fibre tests.

## 2 ANALYSIS OF THE TENSILE FAILURE MODES OF COMPOSITE MATERIALS

### 2.1 Introduction

The high tensile strength and high stiffness of the advanced uniaxial fibrous composites loaded in the fibre direction is well known and up to now has been utilized on a small scale. However, the understanding of the failure mechanisms is limited and it is evident that the failure process is extremely complex. Even when it is assumed that it is possible to fabricate composites with "constant" properties, the failure mechanism remains complex. The complexity is primarily caused by the fact that the strength of the fibres is not constant and this means that the fibres in a composite will not be loaded to their ultimate stress at the same time. The weakest fibres will break first and this introduces the contribution of stress concentrations in the adjacent fibres, to the failure mechanism. In turn the stress concentrations are dependent on the matrix properties and the interface strength.

In this section the various existing tensile failure analyses for unidirectional composites will be discussed. Most of them are based on the fibre strength distribution.

Before discussing the different failure modes of u.d. composites, the statistics of fibre strength and bundle strength will be reviewed.

### 2.2 Fibre strength distribution (Refs.6, 7, 8)

In filament reinforced materials small diameter and high strength and stiff fibres are used. These fibres contain more or

less severe flaws and imperfections. Most high strength materials are brittle and the strength of the individual fibres has to be analysed using statistical methods. The obtained information can be used then, to predict the strength of a multi filament composite material. However, a word of caution has to be said about applying the frequently used "rule of mixtures" to estimate strength. According to this rule, the strength of a composite is the weighted average of the failure stresses in the components. This means that, when the mean strength of the individual fibres is  $\bar{\sigma}_f$  and the filaments occupy an area  $V_f$ , and the influence of the matrix is neglected, the composite strength will be  $\sigma_{\text{comp}} = \bar{\sigma}_f \cdot V_f$ .

Now the possible statistical distribution functions for single filament strength will be considered. In figure 1a the distribution function for brittle fibres is shown and in figure 1b the distribution function for fibres having a strength characterized by a Dirac delta function distribution (perfect fibres). Only for fibres with a distribution function like the one in figure 1b, the rule of mixtures is suitable. This type of fibre distribution is approximated to reasonably well by cold drawn high strength metal wires which generally have a uniform strength. For those fibres which have a broad statistical distribution function such as glass, boron, and carbon fibres, it must be expected that the behaviour of composites can be described only on a statistical basis. The rule of mixtures may overestimate the composite strength for this kind of fibres.

The most widely used expression for the variation of tensile strength of a population of fibres is the Weibull distribution,

$$f(\sigma) = L\alpha\beta^{\beta-1} \exp(-L\alpha\sigma^\beta) \quad (2.2.1)$$

where  $f(\sigma)$  is the probability density function

$L$  is the fibre length

$\sigma$  is the fibre strength

$\alpha, \beta$  are statistical parameters

The length dependence of the strength of brittle fibres is also conveniently described by the Weibull distribution. Long brittle fibres are weaker than short brittle fibres on account of the greater probability of imperfections. This strength-size effect can also be described by the equation

$$\frac{\sigma_1}{\sigma_2} = \left(\frac{l_2}{l_1}\right)^{1/\beta} \quad (\text{Ref. 7})$$

In figure 2,  $f(\sigma)$  is plotted for several values of  $\beta$  while keeping  $L=1$  and  $\alpha=1$ . The Weibull distribution will not reduce exactly to a normal curve but  $f(\sigma)$  approximates very closely to it for values of  $\beta$  around 3.4.

The constant  $\beta$  is an inverse measure of the dispersion of fibre strength. Values of  $\beta$  between 2 and 5 correspond to brittle fibres whereas a value of 20 is appropriate for a ductile cold drawn fibre.

The  $k$ -th moment,  $E(\sigma^k)$ , of the mentioned statistical distribution function defined by;

$$E(\sigma^k) = \int_0^{\infty} \sigma^k f(\sigma) d\sigma, \quad (2.2.2)$$

can be used to define the mean fibre strength:

$$\bar{\sigma}_f = \mu = E(\sigma) \quad (2.2.3)$$

and the variance

$$\text{var} = s^2 = [E(\sigma^2) - \mu^2] \quad (2.2.4)$$

Substitution of equation (2.2.1) in equation (2.2.3) and (2.2.4) yields,

$$\bar{\sigma}_f = (\alpha L)^{-1/\beta} \Gamma\left(1 + \frac{1}{\beta}\right) \quad (2.2.5)$$

and

$$s = (\alpha L)^{-1/\beta} \left[ \Gamma\left(1 + \frac{2}{\beta}\right) - \Gamma^2\left(1 + \frac{1}{\beta}\right) \right]^{1/2} \quad (2.2.6)$$

The coefficient of variation, c.v., for this distribution is given by,

$$\text{c.v.} = \frac{s}{\sigma_f} = \frac{\left[ \Gamma\left(1 + \frac{2}{\beta}\right) - \Gamma^2\left(1 + \frac{1}{\beta}\right) \right]^{1/2}}{\Gamma\left(1 + \frac{1}{\beta}\right)} \quad (2.2.7)$$

The values of the Weibull parameters  $\alpha$  and  $\beta$  can be determined directly from the experimental data and the equations (2.2.5) and (2.2.7).

According to reference 7, the coefficient of variation can be approximated to excellently by  $\text{c.v.} = \beta^{-0.92}$  for the range  $0.05 < \text{c.v.} < 0.5$ . A fair approximation is given by  $\text{c.v.} = \frac{1.2}{\beta}$ . These approximations are convenient for rule of thumb estimates. The curve of  $\text{c.v.} = \beta^{-0.92}$  is shown in figure 3.

### 2.3 Bundle strength (Ref.9)

In section 2.2 it has been discussed how fibres with a scatter in fibre strength can be characterized by a statistical function, the Weibull distribution function. When the distribution function of the single fibres has been determined, the breaking strength of a bundle of fibres can be developed from the statistical weakest link theory.

Consider a bundle composed of a very large number of fibres  $N$  of equal length and the same cross-sectional area. When loading the bundle, at each moment all unbroken fibres have the same elongation. First the weakest fibres will break in succession, and bundle failure will occur when the remaining fibres can no longer sustain the total load. After bundle break the average fibre strength at failure can be obtained from the breaking load and the initial number of fibres. For very large  $N$ , the distribution of the average fibre strength at bundle failure can be approximated to by a normal distribution with mean value or expectation,

$$\bar{\sigma}_B = \sigma_m \left\{ 1 - F(\sigma_m) \right\} \quad (2.3.1)$$

and standard deviation

$$\psi_B = \sigma_m \left\{ F(\sigma_m) \left[ 1 - F(\sigma_m) \right] \right\}^{1/2} \cdot N^{-1/2} \quad (2.3.2)$$

where  $F(\sigma_m)$  is defined with the aid of the cumulative distribution function as:

$$F(\sigma_m) = \int_0^{\sigma_m} f(\sigma) d\sigma \quad (2.3.3)$$

where  $\sigma_m$  is the maximum fibre stress.

The maximum failure stress  $\sigma_m$  is found from the condition that at failure the load borne by the fibres is a maximum. Thus,

$$\frac{\partial}{\partial \sigma} \left\{ \sigma \left[ 1 - F(\sigma) \right] \right\}_{\sigma=\sigma_m} = 0 \quad (2.3.4)$$

When the cumulative distribution function associated with the Weibull function is substituted in equation (2.3.4), the actual stress in each unbroken fibre at bundle failure,  $\sigma_m$ , becomes:

$$\sigma_m = (L\alpha\beta)^{-1/\beta} \quad (2.3.5)$$

The expected value of mean fibre stress at bundle failure is obtained by substitution of equation (2.3.5) in equation (2.3.1)

$$\bar{\sigma}_B = (L\alpha\beta)^{-1/\beta} \exp\left(-\frac{1}{\beta}\right) \quad (2.3.6)$$

The mean fibre stress at bundle failure can be compared with the average tensile strength of the component filaments (Eq.2.2.5)

$$\frac{\bar{\sigma}_B}{\bar{\sigma}_f} = \frac{\beta^{-1/\beta} \exp\left(-\frac{1}{\beta}\right)}{\Gamma\left(1 + \frac{1}{\beta}\right)} \quad (2.3.7)$$

From equation (2.2.7) it follows that the coefficient of variation depends only on the material parameter  $\beta$  and therefore,

the strength efficiency  $\frac{\sigma_B}{\sigma_f}$  can be plotted as a function of the c.v. (Fig.4). When the coefficient of variation is zero (a Dirac delta distribution function), the mean fibre stress at bundle failure equals the mean fibre strength.  $\frac{\sigma_B}{\sigma_f}$  decreases monotonically with increasing c.v.

A unidirectional composite contains a very large number of filaments and the composite strength might be described by the bundle strength, neglecting the influence of the matrix on the failure mechanism. This will be applied in section 3.3.

#### 2.4 Strength prediction of composites, based on fibre strength distribution

In this chapter the existing fracture modes and the related strength predictions will be discussed. In succession, the weakest link failure, the cumulative failure and the fibre break propagation failure is analysed. Although, the strength prediction according to the rule of mixtures is not based on a fibre strength distribution function with a considerable standard deviation it will be treated for completeness and also while this strength prediction method is still widely used for advanced composites.

##### Rule of mixtures

When a composite contains a specified volume fraction of continuous fibres the ultimate tensile strength will be reached when the fibres break. During loading the strain in the fibres and the matrix is the same. The ultimate tensile strength of a composite can be described according to the R.O.M. by the simple equation

$$\sigma_c = \sigma_f \cdot V_f + \sigma'_{ma} (1 - V_f) \quad (2.4.1)$$

where  $\sigma_f$  is the ultimate tensile strength of the fibres  
 $\sigma'_{ma}$  is the tensile stress borne by the matrix when the composite is strained to its breaking point  
 $V_f$  is the volume fraction of fibres

From section 2.2 it is known that (Eq.2.4.1) is suitable only if there is no variation in fibre strength, and if the fibre strength is not dependent on the testing length. For fibres with a scatter

in strength,  $\sigma_f$  equals to the mean fibre strength  $\bar{\sigma}_f$  of a population of tested single fibres. The predicted composite strength is usually handled as an upper bound.

#### Weakest link failure (Ref. 10)

The scatter in fibre strength may have a significant influence on the strength of fibre reinforced materials. When a composite is loaded, the first fibre break will occur at a stress level which will be below the average ultimate tensile strength of the fibres. It is possible that such a fibre break causes a stress wave or initiates a crack in the matrix that results in stress concentrations at the location of the adjacent fibres. In turn the failure of these fibres might cause a catastrophic composite failure. Thus the occurrence of one or a small number of isolated fibre breaks can lead to a type of failure which is called the weakest link mode of failure. This type of failure has been reported by Friedman (Ref. 11) for boron/epoxy composites.

The lowest stress at which this type of failure can occur, is the stress  $\sigma_w$  at which the first fibre will break. It will be clear that, if conditions do not favour the weakest link failure mode, the occurrence of the first fibre break is a necessary but not a sufficient condition for failure. The expected stress at which the first fibre break will occur is therefore a lower bound of the expected composite strength.  $\sigma_w$  can be calculated from the fibre strength distribution function and the number of fibres in the composite.

Consider a population of fibres of length  $L$  whose strength is characterized by the Weibull probability density function  $f(\sigma)$  and the cumulative distribution function  $F(\sigma)$ . For  $N$  fibres, drawn from the given population, the probability density function for the strength of the weakest fibre is given by:

$$p(\sigma) = N \cdot f(\sigma) \left[ 1 - F(\sigma) \right]^{N-1} \quad (2.4.2)$$

The expression for the stress  $\sigma_w$ , at which the first fibre break is expected to occur is obtained by differentiation of equation (2.4.2) and substitution of the functions

$$f(\sigma) = L\alpha\beta^{\beta-1} \exp(-L\alpha\sigma^\beta)$$

$$F(\sigma) = \int f(\sigma) d\sigma = 1 - \exp(-L\alpha\sigma^\beta)$$

$$\Rightarrow \boxed{\sigma_w = \left(\frac{\beta-1}{NL\alpha\beta}\right)^{1/\beta}} \quad (2.4.3)$$

The  $\sigma_w$  value depends strongly on the specimen dimensions. With increasing specimen size, the value of  $\sigma_w$  decreases. For composite materials in realistic structures application of the weakest link strength will lead to a very low allowable design strength. The weakest link strength can be compared with the bundle strength derived in section (2.3). The ratio of the weakest link strength to the bundle strength as a function of the coefficient of variation is presented in figure 5, where

$$\frac{\sigma_w}{\sigma_B} = (\beta-1)^{1/\beta} \cdot N^{-1/\beta} \cdot \exp \frac{1}{\beta} \quad (2.4.4)$$

When c.v. is zero, the weakest link strength equals the bundle strength. Increasing fibre strength scatter results in a decreasing ratio of  $\frac{\sigma_w}{\sigma_B}$ .

On account of this theoretical comparison it can be concluded that the presence of the matrix may impair the strength properties of the composite by producing stress concentrations in the adjacent fibres. In a bundle the load of a broken fibre is equally distributed among the unbroken fibres. It is clear that the weakest link failure must be prevented since the full potential of the fibres cannot be realized in this failure mode.

#### Cumulative weakening failure (Refs.12 to 16)

Rosen (Refs.13, 15) developed the cumulative weakening model for composite failure. In this model, the tensile strength problem has been treated in an approximate fashion by idealizing the fibrous composite into a statistical model in which the statistical information obtained from single fibre tests can be used.



When the weakest link failure does not occur, the load on the composite can be increased and individual fibres will break randomly in the material and in dependence on the applied stress level. A fibre break will be accompanied by a separation of the fibre ends, and stresses in the matrix and at the matrix interface are introduced. Over a specified fibre length there is a reduced stress and there the fibre cannot carry the applied load effectively. This length is called the ineffective length  $\delta$ . The ineffective length is a measure of the portion of fibre which experiences a considerable reduction in stress and can be defined as the value at which the stress reaches some fraction,  $\phi$ , of the undisturbed fibre stress.

In the failure model of Rosen, the composite is composed of a number of layers with thickness  $\delta$ . If a fibre breaks within such layer, no load can be transferred by that fibre, over the layer thickness  $\delta$ . The released load is supposed to be uniformly distributed among the unbroken fibres in that layer. Fibres continue to break till a layer in the cross section is so weakened that it can no longer sustain the applied load. In figure 6 the composite failure according to the cumulative weakening model is presented schematically for a two dimensional material.

The stress level at which the final failure occurs can be determined. The calculation is based on the following assumptions.

- 1 The cylindrical fibre segments of length  $\delta$  consist of identical volume elements subjected to a uniform tensile stress.
- 2 The tensile strengths of the segments are independent of each other and fracture does not propagate from one segment to the adjacent segment.

A fibre segment in a layer can be considered as a link in a chain (the total fibre) and the links of length  $\delta$  can be characterized by a strength distribution function. Each layer consists of a bundle of such links and the composite in turn is then a series of such bundles. The number of layers is determined by the fibre length (or specimen length) and  $\delta$ , so  $n = \frac{L}{\delta}$ . The properties of the total fibre can be described in conformation with section 2.2 by

$$f(\sigma) = L\alpha\beta^{\beta-1} \exp(-L\alpha\sigma^\beta) \quad \text{and} \quad F(\sigma) = \int f(\sigma)d\sigma = 1 - \exp(-L\alpha\sigma^\beta)$$

The distribution function  $g(\sigma)$  of the links and the associated cumulative distribution  $G(\sigma)$  are given by,

$$g(\sigma) = \delta\alpha\beta^{\beta-1} \exp(-\delta\alpha\sigma^\beta) \quad (2.4.5)$$

$$G(\sigma) = \int_0^\sigma g(\sigma')d\sigma' = 1 - \exp(-\delta\alpha\sigma^\beta) \quad (2.4.6)$$

In section 2.3 it has been reported that the bundle strength for a large number of fibres  $N$  can be approximate to by a normal distribution. Because the layer strength is identical to the bundle strength, it can also be described by a normal distribution. The composite is now a chain with elements whose strength properties can be characterized by a normal distribution with  $\omega(\sigma)$  and  $\Omega(\sigma)$ . For  $n$  layers the probability density function for the strength of the weakest layer is given by:

$$\lambda(\sigma_{cb}) = n \cdot \omega(\sigma) \left[ 1 - \Omega(\sigma_{cb}) \right]^{n-1} \quad (2.4.7)$$

where,

$$\Omega(\sigma_{cb}) = \int_0^{\sigma_{cb}} \omega(\sigma)d\sigma$$

A sketch of the three dimensional composite is shown in figure 7. The most probable failure stress is obtained from equation (2.4.7) by differentiation,

$$\frac{d\lambda(\sigma_{cb})}{d\sigma_{cb}} = 0 \quad (2.4.8)$$

which can be written in the form

$$(n-1) \omega^2(\sigma_{cb}) = \omega'(\sigma_{cb}) \left[ 1 - \Omega(\sigma_{cb}) \right] \quad (2.4.9)$$

After substitution of the properties  $\omega(\sigma)$  and  $\Omega(\sigma)$  of the normal distribution in equation (2.4.), the most probable value of the

smallest strength in a sample of size  $n$  is given by

$$\sigma_{cb} = \mu - s(2 \ln n)^{1/2} + \frac{s \ln \ln n + \ln 4N}{2(2 \ln n)^{1/2}} \quad (2.4.10)$$

When the composite dimensions are large, so that there are a large number of layers, the dispersion in the smallest value  $\sigma_{cb}$  is negligible ( $s \rightarrow 0$ ) and the cumulative weakening stress is given by,

$$\sigma_{cum} = \mu = (\alpha \delta \beta)^{-1/\beta} \exp\left(-\frac{1}{\beta}\right) \quad (2.4.11)$$

A comparison between equation (2.4.11) and equation (2.3.6) shows that  $\sigma_{cum}$  is equal to the mean strength of the bundle of fibres of length  $\delta$ .

In figure 8 the ratio  $\sigma_{cum}$  to the mean strength of individual fibres of length  $L$ , is plotted as a function of the coefficient of variation of the mean fibre strength, for various values of  $\delta$ . It is shown that for large values of  $\frac{L}{\delta}$  the composite strength becomes larger than the mean fibre strength. Notice that the composite strength according to the given equation, is independent of the specimen dimensions.

#### Fibre break propagation mode

In the cumulative failure mode, Rosen assumed that after the random fibre breaks, the fibre load is uniformly distributed among the fibres in that cross-section of the specimen. Zweben Ref.13 developed a model in which the influences of load concentrations in the adjacent fibres is taken into consideration. If the weakest link mode of failure does not occur, each fibre break results in a local disturbance of the stress field and the surrounding fibres are subjected to load concentrations which increase the probability that they will break. The number of scattered fibre breaks in the composite becomes larger with increasing load and so do the load concentrations. The stress at which failure of an overloaded fibre leads to subsequent failure of similarly overloaded fibres without an increase of the load, is a measure of the strength in this mode of failure.

In the following section a brief description is given of the calculation of the fibre break propagation stress. In order to calculate the composite strength according to the fibre break propagation mode, it is assumed that the composite consists of a series of layers of elements with axial length  $\delta$ . A composite of length  $L$  that contains  $N$  fibres will have  $\frac{L}{\delta} = n$  layers and a total of  $n \cdot N$  elements (the same assumptions and symbols as in the previous section).

The strength of the elements can be characterized again by  $f(\sigma)$  and the cumulative distribution function  $F(\sigma)$ . ( $F(\sigma)$  is the probability that an element will fail at a stress level  $\sigma$ ). The number of elements in a group of  $n \cdot N$  elements that will fail at a stress level  $\sigma$  is then,

$$E_1 = n \cdot N \cdot F(\sigma) \quad (2.4.12)$$

where  $E_1$  is the number of broken elements at a stress level  $\sigma$ . Under the assumption that in a flat plane the load concentrations in the two adjacent elements are identical, the probability that an element will fail due to the load concentration is given by

$$F(K_i \sigma) - F(\sigma) \quad (2.4.13)$$

where  $K$  is a load concentration factor and index  $i$  is related to the number of broken elements (Appendix I).

Given that a single element is broken, the probability that one, and only one, of the two adjacent fibres will break due to the load concentration is,

$$p(A \cup B) = p(A) + p(B) - p(A \cap B)$$

or

$$p_{2/1} = 2 \left[ F(K_1 \sigma) - F(\sigma) \right] - \left[ F(K_1 \sigma) - F(\sigma) \right]^2 \quad (2.4.14)$$

since the probability that the adjacent fibres will break simultaneously can be described by

$$p(A \cap B) = p_{3/1} = \left[ F(K_1 \sigma) - F(\sigma) \right]^2 \quad (2.4.15)$$

If one of the overloaded fibres adjacent to the broken element, is broken, the two fibres adjacent to the two broken elements will be subjected to a stress level  $K_2\sigma$ . One of these overloaded fibres has previously sustained a stress level  $K_1\sigma$  and the other one only a stress level  $\sigma$ . The probability that one of those fibres will break is,

$$p_{3/2} = \left[ F(K_2\sigma) - F(K_1\sigma) \right] + \left[ F(K_2\sigma) - F(\sigma) \right] - \left[ F(K_2\sigma) - F(K_1\sigma) \right] \cdot \left[ F(K_2\sigma) - F(\sigma) \right] \quad (2.4.16)$$

So the probability of having  $i$  broken fibres given that  $j$  are already broken can be expressed by,

$$p_{i/j} = \text{Function}(K_i, \sigma) \quad (2.4.17)$$

It is now possible to deduct an expression for multiple fibre breaks in the composite in its entirety by using equation (2.4.12) to (2.4.17).

The probability that in the composite material there is at least one fibre fracture is then given by,

$$P(A) = 1 - P(A^c)$$

or

$$P_1 = 1 - (1 - p_1)^{n \cdot N} \quad (2.4.18)$$

where  $A$  is an event

$A^c$  is the complement of  $A$

The occurrence that a given element will break, followed by the fracture of at least one adjacent element but no more than two is,

$p_2$  = probability of one fracture  $\times$  probability of at least one fibre break under condition that one fibre was already broken

$$p_2 = F(\sigma) \cdot (p_{2/1} + p_{3/1}) \quad (2.4.19)$$

The expected number of groups of at least two broken fibres will be then,

The expected number of groups of at least two broken fibres will be then,

$$E_2 = n \cdot N \cdot p_2 \quad (2.4.20)$$

The probability that there is at least one such group is equal to

$$P_2 = 1 - (1 - p_2)^{n \cdot N} \quad (2.4.21)$$

In general

$$E_i = n \cdot N \cdot p_i \quad (2.4.22)$$

$$P_i = 1 - (1 - p_i)^{n \cdot N} \quad (2.4.23)$$

The expected number of groups of fractures can be plotted as a function of the applied stress provided that the fibre strength characteristics and the load concentration factor are known. In figure 9 (Ref.12), the experimental ranges of failure have been compared with the fibre break propagation mode of failure and the cumulative weakening theory. The number of multiple fractures increases rapidly in the range of failure.

It is shown that the curves of  $E_2$ ,  $E_3$  and  $E_4$  are close together and enter the zone of the experimental failures in an early stage. This indicates that fibre break propagation is expected to occur after a small group of multiple fibre breaks.

A conservative prediction of the composite failure load can be based on the first multiple fibre break and can be calculated from

$$E_2(\sigma) = 1 = n \cdot N \cdot p_2 \quad (2.4.24)$$

or

$$n \cdot N \cdot F(\sigma) \cdot 2 \left[ F(K_1 \sigma) - F(\sigma) \right] = 1 \quad (2.4.25)$$

Experimental verification of this failure mode is discussed in reference 13 for continuous glass fibres and boron fibres in an epoxy matrix. The groups of multiple fibre fractures were counted on films of the tests with the specimen under tensile loading. The specimens consisted of one layer only. Figure 10 shows the number

of fibre breaks as a function of the applied load for a number of glass epoxy composites. The calculated number of single broken elements is presented by the dashed line. In the range of the higher loads, the agreement of the number of counted breaks and the theoretical number of breaks is fairly good.

2.5 Summary of strength predictions according to the discussed failure modes

In the previous section the various existing failure modes have been discussed. It was shown that the composite strength can be predicted by;

a the rule of mixtures

$$\sigma_{\text{comp}} = \bar{\sigma}_f V_f + \sigma_{\text{ma}}' (1 - V_f) \quad (2.5.1)$$

b the bundle strength

$$\sigma_{\text{comp}} = V_f \cdot \bar{\sigma}_B = V_f \cdot (L\alpha\beta)^{-1/\beta} \exp(-\frac{1}{\beta}) \quad (2.5.2)$$

c the weakest link strength

$$\sigma_{\text{comp}} = \sigma_w = \left(\frac{\beta-1}{NL\alpha\beta}\right)^{1/\beta} \quad (2.5.3)$$

d the cumulative weakening model

$$\sigma_{\text{comp}} = \sigma_{\text{cum}} \cdot V_f = V_f (\alpha\delta\beta)^{-1/\beta} \exp(-\frac{1}{\beta}) \quad (2.5.4)$$

e the fibre break propagation model, where the stress at first multiple fibre break can be calculated

$$(2.5.5)$$

from:

$$n \cdot N \cdot F(\sigma) \cdot 2 \left[ F(K_1 \sigma) - F(\sigma) \right] = 1$$

The contribution of the matrix properties to the composite strength according to the ROM can be neglected. An approximation of the composite strength by the bundle strength can be expected when complete fibre debonding occurs, (low fibre-matrix interface strength). For the deduction of the weakest link strength it was assumed that the first fibre break would produce a stress wave. This implies that a stiff matrix and a strong interface bond will contribute to this failure mode.

In the cumulative weakening model, the matrix properties determine the magnitude of the ineffective length. Inelastic effects and fibre-matrix debonding however, are not incorporated in this strength prediction. Weaker interface strength (larger ineffective length) will result in a lower composite strength.

Just as in the weakest link model, the load concentration factor used in the fibre break propagation model is determined by the matrix properties. In equation (2.5.5), the load concentration factor is based on elastic matrix properties. In reality the visco-elastic behaviour of the matrix and fibre-matrix debonding reduce the load concentration factor and therefore the calculated stress at first multiple fibre break will be a lower bound.

The strength prediction based on the discussed failure criteria will be compared with experimental results obtained by tensile tests on boron/epoxy and carbon/epoxy specimens.

### 3 EXPERIMENTAL RESULTS

#### 3.1 Mechanical properties of the fibres

Since the theoretical composite strength predictions are based on fibre strength, the strength of the reinforcing fibres has to be determined. Two types of strong fibres were investigated, 1 the high strength carbon fibre Grafil HT-S from Courtaulds 2 the boron fibre fabricated by N.V. Philips Eindhoven. The carbon fibres were delivered as continuous tow consisting of 10.000 filaments. One part of the tow was sized and the other part was unsized. A size is usually applied in order to improve the winding properties.

The tensile strength of single carbon fibres was determined in a universal Instron testing machine (2N load cell), and partially in a special fibre testing machine, the Fafegraph. The gauge length of the tested carbon fibres was 10 and 30 mm for the Fafegraph tests and 50 mm for the Instron tests. The tested fibres were selected at random from the continuous tow.

The way of clamping the fibres in the two test machines was different. In the Fafegraph the carbon fibres were tightened between



hard-rubber wheels. In order to test the fibres in the Instron, they were mounted on a paper frame with a cut-out corresponding to the desired gauge length (50 mm). This is illustrated in figure 11. In the frame holes have been drilled in order to apply a uniaxial tensile load. After fixing the frame in the grips of the testing machine, both sides of the frame are cut which results in only the fibre being loaded. The cross head speed was 2 mm/min and a load-strain curve was simultaneously plotted on an X-Y recorder (Fig.12).

The strength properties of the carbon fibres are presented in the shape of a histogram in figure 13. Also the mean fibre strength and standard deviation are mentioned. On account of the Fafegraph tests it can be concluded that there is a length-strength dependence. Furthermore there is an evident difference in strength between the unsized and sized fibres. The higher strength of the sized fibres can be attributed to the beneficial action of the size which protects the fibre against surface damage. In figure 14 the length-strength dependence is plotted. The 95 % -confidence interval for the mean was calculated under the assumption that the fibre strength distribution could be characterized reasonably well by a normal distribution.

If there is a linear relation between the fibre length and the strength, the expected mean strength value at a gauge length of 50 mm would be about  $10.5 \cdot 10^{-2}$  N (on account of the Fafegraph tests). However, the strength of sized fibres as well as the strength of the unsized fibres were higher. This discrepancy can be attributed to different clamping methods. Probably, the rubber grips of the Fafegraph are harmful for the mean fibre strength, and cause failure in the clamped area. This phenomenon could not be established well since fibre break is attended by shatter of the fibre in its entirety.

The average diameter of the carbon fibres was determined from optical measurements of 30 unsized fibres. In calculating the failure stresses it was assumed, that the influence of scatter in fibre diameter was small in comparison with the influences of material imperfections on the fibre strength.

The fibre strength could be characterized by a Weibull distribution function  $f(\sigma)$ , and the material parameter  $\beta$  of that function was determined from the experimental test data and the theory of section 2.2.

A survey of test data of fibres with gauge length 50 mm is shown in table 1. The strength properties measured correspond well with the properties determined by the manufacturer. However, the scatter in fibre diameter was larger than quoted.

For testing the boron fibres the single fibres with a gauge length of 50 mm were mounted on 0.5 mm thick sheets with a strain gauge adhesive, figure 11.

A histogram of the test results is presented in figure 15. The peculiar shape of this histogram may be caused by the presence of two kinds of fibre defects, each resulting in a specific strength distribution. The fibre defects can be surface imperfections and internal flaws. The calculated mean fibre strength corresponded well with the strength data, given by the manufacturer. The scatter in fibre diameter was small.

### 3.2 Mechanical properties of bundles

Bundle tests have been performed on carbon tow in the unsized- and sized condition. This tow is the starting material for the winding process in order to fabricate prepreg material. For quality control bundle tests can be used. The main problem of testing bundles will be, fixing the bundle ends in a way that at each moment all unbroken filaments have the same elongation. The set up to produce adequate specimens is shown in figures 16 and 17. A vacuum cleaner was used to stretch the bundle uniformly. Two moulds, mounted on a plate by a weak adhesive, were put around the stretched untwisted tow and were filled with Araldit resin. The mould end plates were sealed with felt impregnated with wax. Tensile tests were performed in a 500 kgf Amsler testing machine after the supporting plate was removed, with the filled moulds serving as loading tabs. The gauge length was 50 mm. The results of the bundle tests are presented in table 2. As could be expected, the mean bundle strength of the sized tow was higher than the mean strength of the unsized tow. When the experimental bundle strength is compared with the mean fibre strength of single fibres, it appears that the mean fibre strength at bundle failure is about 61 % of the mean fibre strength of a population of single fibres. On account of the determined coefficient of variation, a percentage of about 70 % was expected (Fig.4). This discrepancy can

be attributed to incorrect alignment of the fibres, non uniform load introduction and abrasion of the individual fibres during handling of the bundles. Furthermore, the theoretical bundle strength was derived for fibres having equal diameter. From fibre diameter measurements it was learned that the standard deviation was considerable. So this also may have led to a low bundle strength. On the other hand, the test procedure for bundle tests seems to reproduce well, since the scatter in bundle strength (sized tow) was quite low. Therefore the bundle test can be used for quality control of delivered carbon tow for the winding process, in spite of the bias to low strengths. When in a u.d. composite material the influence of the matrix on the strength properties is neglected, the bundle strength theory can be used for strength prediction. This will be applied to the tested carbon- and boron composites.

### 3.3 Laminate tests

#### 3.3.1 Carbon/epoxy specimens

The carbon composite specimens were fabricated by Fokker-VFW. The reinforcing component was the high strength surface treated fibre, Grafil HT-S from Courtaulds. The matrix/hardener system was Shell DX231/DX137 with the mechanical properties as presented in table 3. Fokker received the material from Fothergill and Harvey in the shape of prepreg sheets with thickness 0.125 mm.

Test specimens have been made in an autoclave at a temperature of 120°C and under a pressure of  $3 \cdot 10^5$  Pa. Three types of specimens were fabricated, consisting of 1, 3 and 9 layers of prepreg. Glass fibre tabs (fibre orientation 0°, ± 45°, 90°) were bonded to the specimen ends in order to clamp the test specimens. The dimensions are shown in figure 18. No waisting was applied in connection with various strength predictions based on the strength distribution of fibres with length 50 mm. Various thicknesses were tested in order to investigate whether there was a thickness-strength dependence. Specimens built up of 3 and 9 layers have been tested in an Amsler testing machine and the one-layer specimens in an Instron testing machine. On several, 3 and 9-layer specimens, strain gauges were mounted to determine the E-modulus. In table 4 the test results are presented of the carbon composite specimens. Various specimens

broke in the clamping area. However, since failure in the grips not always resulted in a lower strength, the concerned data have been used for the mean strength determination. The strength ratio of the 3- and 9-layer specimens corresponded well with the ratio of the number of layers. The strength of the 1-layer specimens remained below expectation, however. This can be explained by the shape of the load-displacement curve, figure 19. During the increasing load, the edges of the specimens splintered prematurely, leaving the centre section of the specimen intact. So the breaking load was borne by a cross section, smaller than the initial cross section. It might be argued that this is inherent to the cumulative weakening and fibre break propagation modes, but the first failures were determined by conditions other than strength variability of the fibres. Another inaccuracy in determining the ultimate prepreg strength is introduced by the determination of the cross sectional area. As can be seen in figure 20 it is very difficult to measure the specimen thickness. Usually the specimen thickness will be determined by measuring the distance between the peaks on the two surfaces of the specimen.

Therefore, the strength data concerning carbon prepreg material as monopley are not believed to be representative for the pure uniaxial carbon prepreg strength and this way of testing prepreg is not recommended to obtain reliable strength data. The failure mode of the monopley specimens was quite different from the failure mode of the thicker specimens. After testing, the monopley specimen was completely splintered, probably due to the release of the stored elastic energy, figure 21.

In order to compare the test results with the various theoretical strength predictions, the fibre volume had to be determined. This has been carried out optically by using a Quantimet apparatus. For that purpose specimens were prepared of one 3-layer specimen and four 9-layer specimens. As can be observed in figure 22 and 23 the single layers are bounded at various locations by resin rich zones and by voids. The mean fibre percentage was determined by scanning the cross section in its entirety. To avoid scratches on the specimen surface which would reduce the measured fibre volume, careful grinding and polishing was carried out. The measured  $V_f$  values are presented in table 5.

3.3.1.1 Comparison of strength data with theoretical strength predictions

The comparison of the test results with the theoretical strength predictions has been restricted to the 9-layer specimens, since the fibre volume fraction of these specimens could be determined with sufficient accuracy. The rule of mixtures, the bundle strength, and the cumulative weakening strength will be considered successively. It was not found to be realistic to compare the carbon/epoxy failure with the weakest link failure mode and the stress at the first multiple fibre break.

Rule of mixtures: (Eq.2.5.1)

$$\begin{aligned}\sigma_{\text{comp}} &= V_f \cdot \bar{\sigma}_f + \sigma'_{\text{ma}} (1 - V_f) \\ &= 0.426 \times 2560 + 25 \times 0.574 = 1100 \text{ N/mm}^2\end{aligned}$$

$$\begin{aligned}E_c &= V_f \cdot E_f + E_m (1 - V_f) \\ &= 0.426 \times 242000 + 2500 \times 0.574 = 104400 \text{ N/mm}^2\end{aligned}$$

Bundle strength; (Eq.2.5.2)

Two strengths values can be used, the bundle strength based on the scatter in strength of single fibre tests and the actually determined bundle strength

$$\begin{aligned}1. \sigma_{\text{comp}} &= V_f \cdot \bar{\sigma}_B \\ &= 0.426 \times 0.7 \times 2560 = 762 \text{ N/mm}^2\end{aligned}$$

$$2. \sigma_{\text{comp}} = V_f \times 0.61 \times 2560 = 665 \text{ N/mm}^2$$

Cumulative weakening strength; (Eq.2.5.4)

$$\sigma_{\text{comp}} = \sigma_{\text{cum}} \cdot V_f = V_f \cdot (\alpha \delta \beta)^{-1/\beta} \exp(-\frac{1}{\beta}) = V_f \times (\frac{\delta}{L})^{-1/\beta} \times \bar{\sigma}_B$$

In order to calculate the cumulative weakening strength, a numerical value for the ineffective length has to be selected. An estimate can be obtained by measuring the fibre pull out at the fracture surface of a tensile failure. Two values will be used,  $\delta=0.5$  and  $\delta=0.2$  mm. The corresponding composite ultimate strength becomes

$$\sigma_{\text{comp}}(\delta=0.5) = 0.426 \times \left(\frac{0.5}{50}\right)^{-1/7.5} \times 0.7 \times 2560 = 1410 \text{ N/mm}^2$$

$$\sigma_{\text{comp}}(\delta=0.2) = 0.426 \times \left(\frac{0.2}{50}\right)^{-1/7.5} \times 0.7 \times 2560 = 1585 \text{ N/mm}^2$$

There is a considerable influence of the ineffective length on the composite strength.

In the following table an overview is given of the strength predictions in comparison with the test result

Theory	Theoretical composite strength	Test result N/mm <sup>2</sup>
R.O.M.	1100	} 1180
Bundle strength 1	762	
Bundle strength 2	665	
Cumulative strength $\delta=0.5$	1410	
Cumulative strength $\delta=0.2$	1585	

### 3.3.2 Boron/epoxy specimens

The boron/epoxy specimens were fabricated from boron prepreg tape. The prepreg material (width 12 mm) with the same matrix as the carbon composite, was delivered by N.V. Philips, Eindhoven. The material consisted of one layer of aligned boron fibres upon a thin fabric of glass fibres.

Tensile specimens were made at the National Aerospace Laboratory, NLR. The curing temperature was 120°C and the applied pressure (by dead weight) about  $0.5 \cdot 10^5$  Pa. Since the edges of the prepreg material were damaged, waisting of the tensile specimens was applied. The number of fibres in the smallest cross section of a prepreg layer was about 66 fibres. Aluminium tabs (1 mm thick) were bonded to the specimen ends. The dimensions are shown in figure 18. The specimens consisted of 1 layer, 3 layer, and 9 layers of prepreg material. Tensile tests were performed in an Amsler testing machine and in an Instron testing machine (for monoply specimens). The test results are presented in table 6. The scatter in strength is considerable.

This can be caused by various effects such as

- 1 clamping effects, non uniform load introduction
- 2 material defects

ad.2 A view of the cross sectional area shows numerous split fibres (Fig.24). This can not all be attributed to the grinding and polishing processes, since at some locations, the matrix resin had flowed between the split fibre ends. Probably fibre degradation occurred during the fabrication process. A Scanning Electron Microscope (SEM) photograph of the fracture surface shows that numerous fibres contain internal flaws, figure 25.

### 3.3.2.1 Comparison of strength data with theoretical strength predictions

Although there was a large scatter in strength properties it was tried to compare the strength data with various strength predictions.

The results have been plotted in figure 26. The marked values of table 6 were not used since they were invalid.

## 4 INFLUENCE OF THE SCATTER IN STRENGTH PROPERTIES ON DESIGN ALLOWABLES AND THE RELIABILITY OF A STRUCTURE (REFS.21 TO 24)

The determination of design allowables of composite materials for structural applications is necessary for an assessment of the load carrying ability of a structure. An aircraft structure must be able to sustain a limit load without excessive deformation or a decrease in stiffness. Furthermore the structure must be capable to withstand an operational fatigue load spectrum and an atmospheric environment during a specified service life.

In this section only the design values concerning the static strength properties will be considered.

The scatter in mechanical properties of composite materials causes the design values to be lower than the mean properties. As seen in previous sections, the composites under uniaxial loading generally exhibit appreciable scatter in strength. This can be attributed to a number of variables that influence the response of the material (production parameters, testing parameters). For a multidirectional material the failure behaviour is even more complex

and it will be difficult to characterize the different influences since,

- different failure mechanisms operate in each major material direction.
- the distribution functions for failure in various directions usually have different material parameters.
- interaction effects cannot be conveniently incorporated.

Usually the assumption is made that failure of multidirectional laminates would be fibre controlled. In order to describe the composite material behaviour under multiaxial loading semi-empirical relationships have been developed (Refs.25, 26) based on the characteristics of the uniaxial material properties.

The design allowable for the unidirectional composite can be obtained from sample tests. Since scatter in properties can be expected, the values have to be related to a specified confidence level. For conventional metals A-values are used (Ref.22), but for composites with a larger coefficient of variation B-values can be employed. This means that 90 percent of a population is expected to fall above this value with a confidence level of 95%, under the assumption that the population can be characterized by a normal distribution. (For A values these numbers are 99% and 95% respectively).

This design value then equals

$$F_a = F_{av} - k.s \tag{5.1}$$

or

$$\frac{F_a}{F_{av}} = 1 - k.cv \tag{5.1}$$

- where  $F_{av}$  is the mean of a number of test data
- $s$  is the standard deviation
- $k$  is the one-sided tolerance factor for the normal distribution at some particular confidence level
- $cv$  is the coefficient of variation

The one-sided tolerance factor  $k$  depends on the number of test data and the chosen probability of survival with a specific confidence level, (Fig.27).



Higher design values will be obtained when it is assumed that the cv of the complete strength distribution is known. In figure 28 a comparison is made between the ratio of design allowable and mean sample strength as a function of the number of tests, with the population cv and sample cv as parameters. Assumed knowledge of the population cv results in a higher design allowable.

According to reference 21, the gathered test data indicate characteristic average cv's for particular simple loading modes, (Tab.7).

By using the average cv's, realistic design allowables will be obtained. However, the designer should not use the given cv without careful appraisal of the data by comparison with data determined by his own materials department. The test results of reference 23 (Tab.8) for instance are quite different from those in table 7.

For combined loading of a laminate the total risk of rupture can be the basis for deducting design allowables in terms of safety factors. The total risk of rupture of a material under combined tension, compression and shear for instance can be described by the sum of risks of rupture under the specified uniaxial tension, compression and shear loadings.

For structures wholly designed in composite materials safety factors can be derived from the safety factor of a conventional metal structure (ultimate load =  $3/2$  limit load) by requiring the same reliability (i.e. risk of failure).

## 5 DISCUSSION

Theoretical strength predictions for unidirectional composite materials have been considered. Tensile tests on carbon/epoxy and boron/epoxy were performed in order to compare the experimental strength data with the theoretical strength predictions.

Concerning the carbon/epoxy composites, it can be concluded that the theory based on the bundle strength underestimates the real strength of the composite considerably. A better approximation was given by the rule of mixtures. It appeared that the strength prediction based on the mean strength of the virgin fibres, was

reasonably well in agreement with the test results. The ROM was even, somewhat conservative.

However, the ROM was applied for specimens and fibres with a gauge length of 50 mm. The question arises at which gauge length the fibre strength has to be determined in order to calculate composite strength for real structural sizes. It is not expected that the strength-length dependence for composite materials is as pronounced as the strength-length dependence of the reinforcing fibres. This aspect requires further study.

There exists a vast body of experience indicating that the ROM gives an accurate prediction of stiffness (Refs.28, 29). This was borne out by the present test results.

The cumulative weakening strength prediction, strongly overestimates the real composite strength. This can be attributed to the following factors;

- the strength prediction is based on a uniform distribution of the fibres in the cross sectional area. As can be seen in figure 29 the specimen cross section does not show an ideal composite material. The presence of voids and resin rich zones were responsible for a nonuniform fibre distribution.
- in the theory it was assumed that the fibres were of equal diameter. From fibre diameter measurements (Tab.1) and figure 20 a considerable variation in fibre diameter was observed.

The weakest link and the fibre break propagation failure mode were not realistic for the same reasons.

It is possible that a better agreement between the cumulative weakening strength and the test results will be reached when void free specimens can be fabricated with uniformly distributed fibres.

Another uncertainty remains, however, which is the magnitude of the ineffective length  $\delta$ . According to reference 16 the  $\delta$  can be computed from the following equation.

$$\delta = \left(\frac{E_f}{G_m}\right)^{\frac{1}{2}} \cdot \left(\frac{1-V_f^2}{2V_f^2}\right)^{\frac{1}{2}} \cdot d_f \quad (5.1)$$

This equation can be used for elastic fracture processes but does not incorporate fibre debonding and plasticity effects. So the obtained  $\delta$  is a minimum value. Generally, the size of the ineffective length, even when inelastic effects are present, is not greater than 100 fibre diameters (Ref.16). For the concerned carbon/epoxy specimens, the  $\delta_{\min}$  was  $12.5 d_f$ . The actual value of  $\delta$  then may be in the wide range between  $12.5 d_f$  and  $100 d_f$  which means that considerable strength differences can be expected.

Furthermore may be questioned, whether the ineffective length is constant throughout the composite material.

The test results of the boron/epoxy specimens exhibited a large scatter. The scatter in strength was so high that the fabrication process was believed to be incorrect. However, after omission of the uncharacteristically low test values, it could be concluded on account of the data in figure 26, that the greater part of the test results was near the bundle strength. The fracture surfaces exhibited features of local debonding, but a complete debonding as would be expected at failure in accordance with the bundle strength was not observed. The ROM, the cumulative weakening strength, and the fibre break propagation strength overestimate the boron/epoxy strength.

## 6 CONCLUSIONS

1. The mean strength and the strength distribution of boron and carbon reinforcing fibres could be determined from single fibre tests.
2. There was a length-strength dependence for the carbon and the boron fibres.
3. The tensile strength of the tested carbon/epoxy specimens could be predicted reasonably well by the rule of mixtures.
4. The tensile strength of the tested boron/epoxy specimens could be described by the bundle strength theory.
5. There is no need to employ the more advanced strength predictions based on the cumulative weakening model and the fibre break propagation model, when the fabricated composite material contains voids and a nonuniform distribution of fibres.

6. Design allowables can be derived from the mean strength and the coefficient of variation of a small sample. More satisfactory allowables, however, can be obtained by using the coefficient of variation, characteristic for a particular loading situation.

7 REFERENCES

- 1 Taig, I.C. Airframe applications of advanced composites.  
AGARD-LS-55, 1972.
- 2 Waddoups, M.E. Composites in the structural design process.  
AGARD-LS-55, 1972.
- 3 Noton, B.R. Potential high-volume applications of advanced composites.  
Composite materials Vol.3 Engineering applications of composites.  
Academic Press New York and London 1974.
- 4 Parmley, P.A. Military aircraft.  
Composite materials Vol.3 Engineering applications of composites.  
Academic Press New York and London, 1974.
- 5 Ashton, J.E.,  
Burdorf, M.L. and  
Olson, F. Design, analysis, and testing of an advanced composite F-111 fuselage.  
Composite materials; Testing and Design  
ASTM STP 497, 1971.
- 6 Weibull, W. A statistical distribution function of wide applicability.  
Journal of applied mechanics, Sept. 1951.
- 7 Robinson, E.Y. Estimating Weibull parameters for materials.  
NASA, Jet propulsion laboratory, California,  
Technical memorandum 33-580, 1972.
- 8 Kelly, A. Fracture phenomena in composites.  
Dritte internationale Tagung über den Bruch  
München, April 1973.

- 9 Coleman, B.D. On the strength of classical fibres and fibre bundles.  
J. of Mech.Ph.Solids, Vol.7, 1958.
- 10 Epstein, B. Statistical aspects of fracture problems.  
J. of Appl. Physics, Vol.19, Feb. 1948.
- 11 Friedman, E. A tensile failure mechanism for whisker reinforced composites.  
22nd Annual meeting of the reinforced plastics division of the SPI, Washington, DC, Feb. 1967.
- 12 Zweben, C. and Rosen, B.W. A statistical theory of material strength with application to composite materials.  
J. Mech.Phys. Solids, Vol.18, 1970.
- 13 Zweben, C. Tensile failure of fibre composites.  
AIAA Journal, Vol.6, no.12, Dec. 1968.
- 14 Rosen, B.W. Tensile failure of fibrous composites.  
AIAA Journal, Vol.2, no.11, Nov. 1964.
- 15 Zweben, C. A bounding approach to the strength of composite materials.  
Eng. Fracture Mech. Vol.4, 1972.
- 16 Rosen, B.W. and Zweben, C. Tensile failure criteria for fibre composite materials.  
NASA CR-2057, 1972.
- 17 Gücer, D.E. and Gurland, J. Comparison of the statistics of two fracture modes.  
J. Mech. Phys. Solids, Vol.10, 1962.
- 18 McMahon, P.E. The relationship between high modulus fibre and unidirectional tensile strength.  
Sampe Quarterly, Oct. 1974.

- 19 Wright, M.A. and Jannuzzi, F.A. The application of the principles of linear elastic fracture mechanics to unidirectional fibre reinforced composite materials. J. Composite materials, Vol.7, Oct. 1973.
- 20 Kreyszig, E. Introductory mathematical statistics. John Wiley and Sons, Inc., New York, London, Sydney, Toronto, 1970.
- 21 Jones, B.H. Determination of design allowables for composite materials. Composite materials: Testing and Design, ASTM STP 460, 1969.
- 22 Hadcock, R.N. Design philosophy for boron/epoxy structures. Composite materials: Testing and Design, ASTM STP 497, 1972.
- 23 Elkin, R.A., Fust, G. and Hanley, D.P. Characterization of graphite fibre/resin matrix composites. Composite materials: Testing and Design, ASTM STP 460, 1969.
- 24 Ashton, J.E. Implications of the behaviour of advanced composite materials. J. Frankl. Inst., Vol.290, 1970.
- 25 Tsai, S.W. and Wu, E.M. A general theory of strength for anisotropic materials. J. Comp. Mat., Vol.5, 1971.
- 26 Sendeckyi, G.P. A brief survey of empirical multiaxial strength criteria for composites. Composite materials: Testing and Design ASTM STP 497, 1972.
- 27 Hedgepeth, J.M. and Van Dijke, P. Stress concentrations from single-filament failures in composite materials. Textile Research Journal, July 1969.



APPENDIX  
LOAD CONCENTRATION FACTOR

When one or more fibres are broken in a u.d. composite material under stress, the load in the broken fibre or fibres must be transferred through the matrix to the adjacent fibres. The created local load concentrations are important for the understanding of the fibre break propagation failure mode in composite materials.

Hedgepeth (Ref.27) analysed the influences of fibre fractures on the static and dynamic load concentrations in a two dimensional and a three dimensional u.d. composite. Hedgepeth used a shear lag model wherein the rate of change of the load in the fibre is equated to the shear forces, transmitted uniformly through the matrix from the adjacent fibres.

The numerical results of his analysis for a two dimensional material are shown in the following table. Besides the static load concentration factor, the dynamic concentration factor, as a consequence of a sudden fibre break, is given.

number of broken fibres	load concentration factor, $K_i$	dynamic overshoot
1	1.33	1.15
2	1.60	1.19
3	1.83	1.20
4	2.03	
5	2.22	
6	2.39	
$\infty$	—	1.27

The load concentration factor  $K_i$  is influenced by the fibre arrangement. For a three dimensional material,  $K_i$  decreases since the broken fibre is surrounded by six unbroken fibres (instead of two) over which the load can be distributed uniformly.

In his model, Hedgepeth assumed that no interfacial debonding and plastic deformation will occur. In a realistic composite material however, there will be debonding over a certain length of the broken fibre ends, resulting in a reduced load concentration factor (Fig.30). This implies that the probability on failure due to load concentrations decreases with increasing ineffective length.



TABLE 1 Mechanical properties of carbon fibres of gauge length 50 mm

	unsized	sized	according to manufacturer $\bar{x}$
mean strength (N) (about 80 fibres)	13.0 * 10 <sup>-2</sup>	15.36 10 <sup>-2</sup>	
C.V.	23 %	15,6	
mean fibre diameter ( $\mu\text{m}$ ) (30 fibres)	8.75		8.9
C.V.	14 %		4.6 %
mean tensile strength N/mm <sup>2</sup>	2170	2560	2100-2800
strain at fibre break	0.9 %	1.07 %	
E-modulus N/mm <sup>2</sup>	240000	242000	225000-280000

$\bar{x}$  Grafil data sheets, Augustus 1970

TABLE 2 Strength data concerning carbon tow consisting of  
10.000 filaments *Bundle test - Tow test*

	unsized	sized
mean strength (N) (8 specimens)	742	932
C.V.	4.6 %	1.3 %
mean fibre strength (N/mm <sup>2</sup> )	1240	1540

TABLE 3 Mechanical properties matrixsystem

	$\sigma_{ult}$ N/mm <sup>2</sup>	$E_m$ N/mm <sup>2</sup>	$\epsilon_{fracture}$ %	ILSS N/mm <sup>2</sup>
Shell DX 231/ DX 137 code 92 (Fothergill and Harvey)	80	2500	7	80

TABLE 5 Fibre volume fraction of 9-layer carbon/epoxy specimens

	$V_f$ (%)
Specimen No. 3	41.46
No. 4	43.88
No. 6	42.58
No. 8	42.50
	mean 42.60

TABLE 4 Tensile strength of carbon/epoxy specimens

Number of layers prepreg	1	3	9
tensile strength N/mm <sup>2</sup>	364	942	1094
	443	981	1097
	476	1025	1134
	484	1088	1143
	500	1145	1171
	606	1183	1212
		1193	1257
		1203	1272
specimen thickness mm	0.17	0.35	1.05
mean tensile strength N/mm <sup>2</sup>	480	1095	1172
CV	16.5 %	9.3 %	5.8 %

TABLE 6 Strength properties of boron epoxy specimens

Number of layers prepreg	1	3	9
tensile strength N/mm <sup>2</sup>	735	{ 245 } x	{ 540 } xx
	735	{ 520 } x	{ 590 } xx
V <sub>f</sub> about 45 %	755	{ 710 } x	670
	770	910	760
	870	1030	815
	910	1050	1000
	910	1060	1040
	940	1180	1070
	950		
	1030		

x specimen torqued due to the fabrication process.

xx these lower strength values are accompanied by delamination near the fracture surface of one side of the specimen which indicate on no pure uniaxial loading.

TABLE 7 Coefficients of variation for various loading modes (Ref. 22)

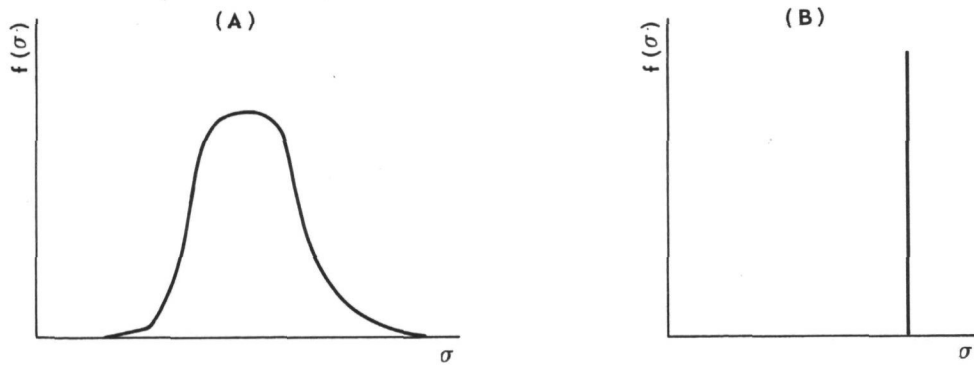
load	coefficient of variation	
	range	average
tension		
longitudinal	0.04 - 0.12	0.10
transverse	0.01 - 0.20	0.11
compression		
longitudinal	0.08 - 0.16	0.12
transverse	0.05 - 0.11	0.08
shear		
in-plane	0.02 - 0.08	0.06
interlaminar	0.02 - 0.08	0.05
flexure		
longitudinal	0.01 - 0.06	0.03
transverse	0.01 - 0.02	0.08
filaments	0.06 - 0.19	0.12

TABLE 8 Coefficients of variation for a number of unidirectional carbon composites (Ref. 23)

material	tension		compression		shear
	longitudinal	transverse	longitudinal	transverse	in-plane
T-50	0.03-0.11	0.07-0.50	0.13-0.33	0.13-0.24	0.02-0.10
M-II	0.02-0.07	0.12-0.20	0.10-0.12	0.05-0.06	0.23-0.35
HMG-50	0.06-0.15	0.23-0.35	0.07-0.10	0.23-0.29	0.22-0.26

T-50 : Thornel-50      HMG-50 : High modulus fibre of HITCO

M-II : Morganite Type II.



**FIGURE 1** Strength distribution functions for fibres with a variable strength and fibres with a unique strength

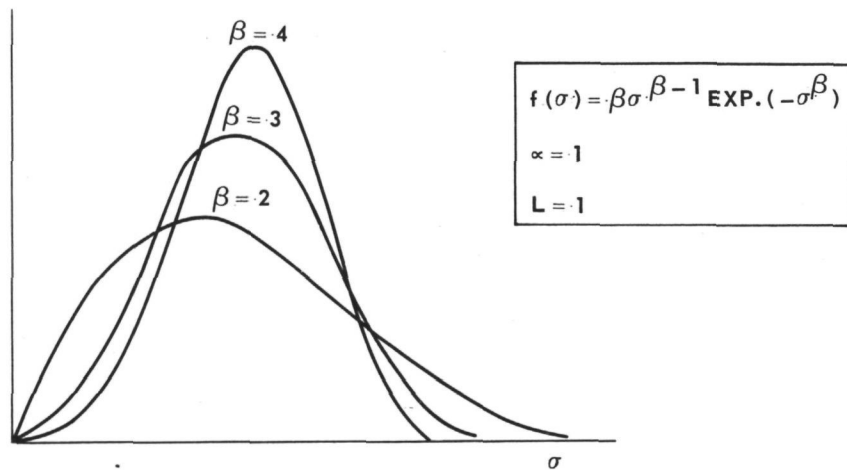


**FIGURE 2** Typical Weibull frequency distribution curves for application as failure probability density factor

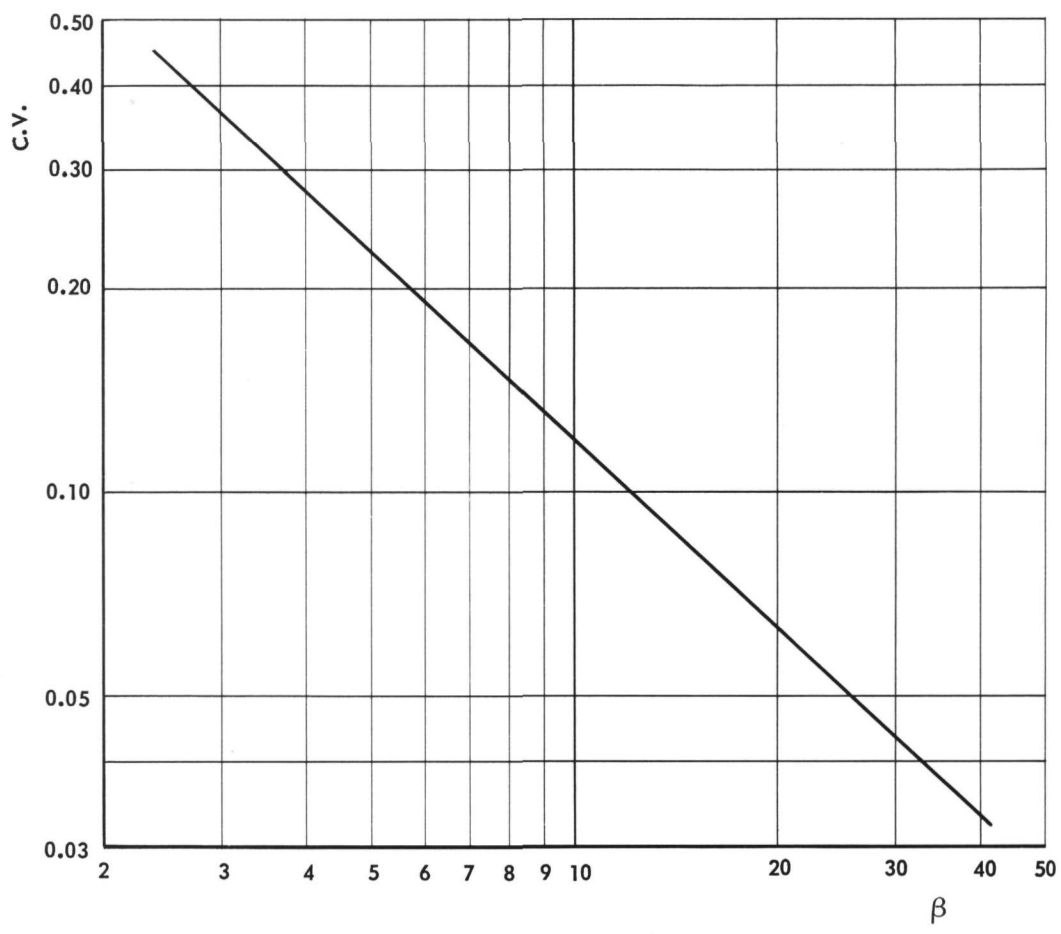


FIGURE 3 The coefficient of variation as a function of the Weibullparameter  $\beta$

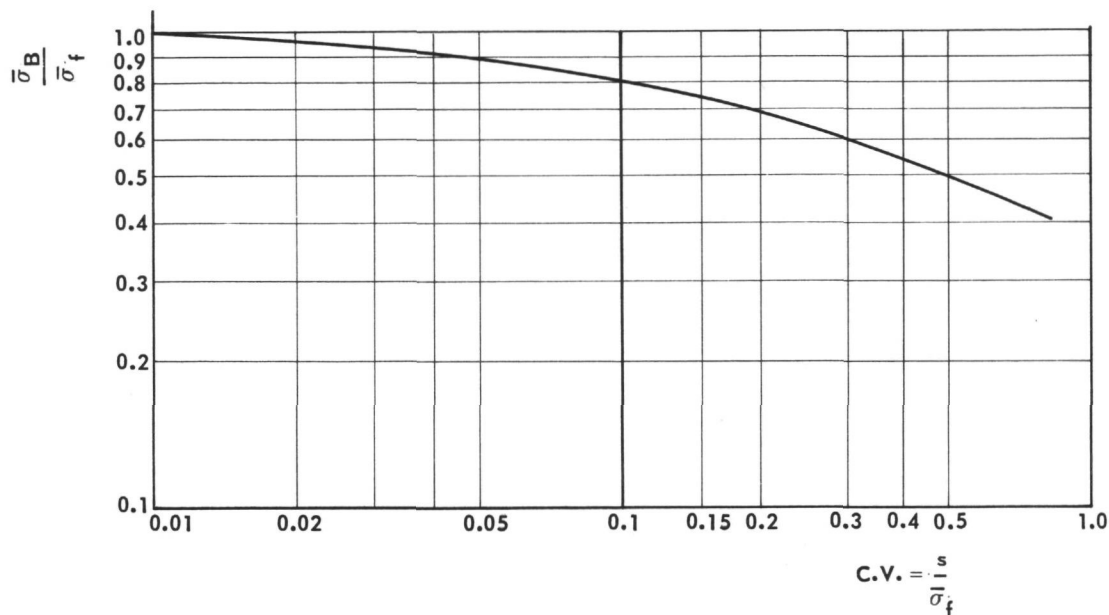


FIGURE 4 The ratio of theoretical bundle stress to mean fibre stress as a function of the coefficient of variation

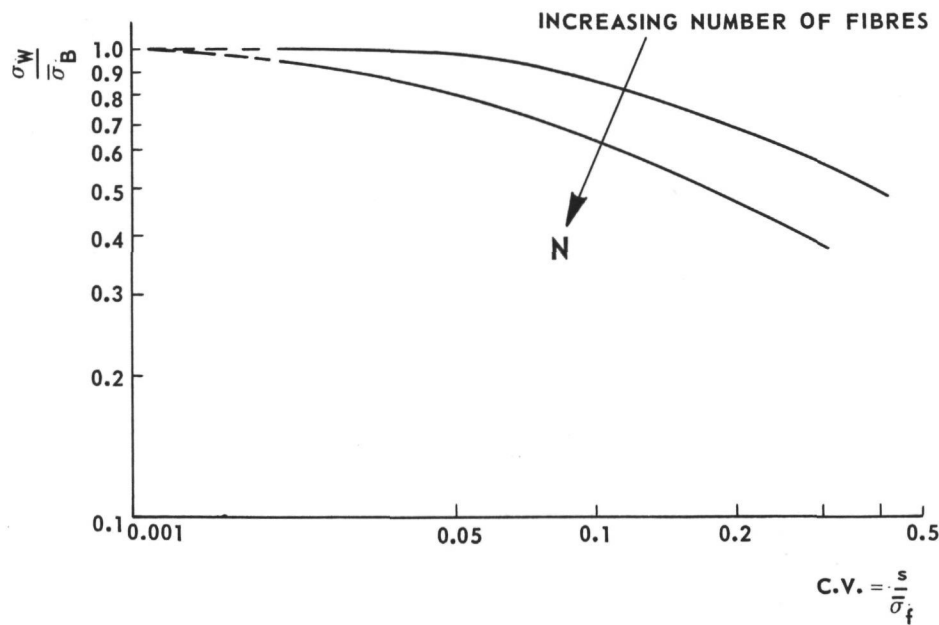


FIGURE 5 The ratio of weakest link stress to the bundle stress as a function of the coefficient of variation



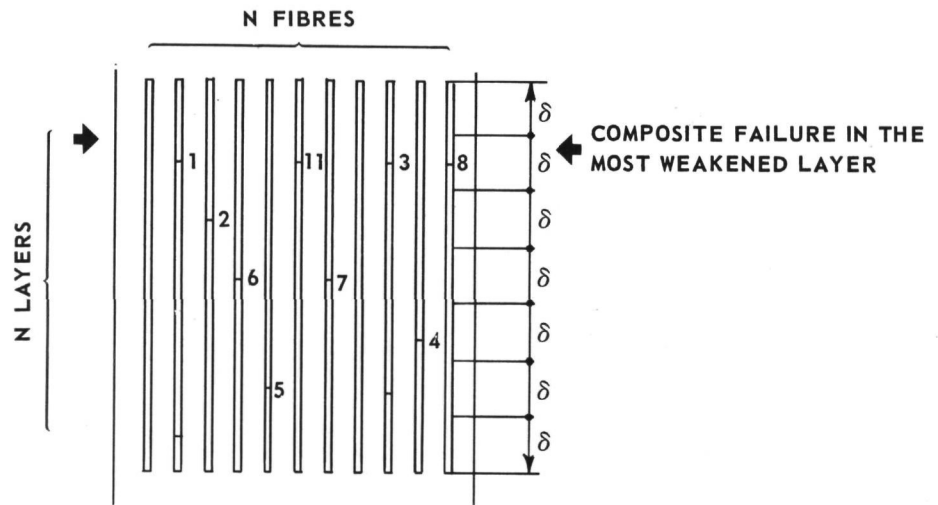


FIGURE 6 The cumulative fracture mode showing fibre fractures randomly in the material until one layer is weakened such, that composite failure will occur

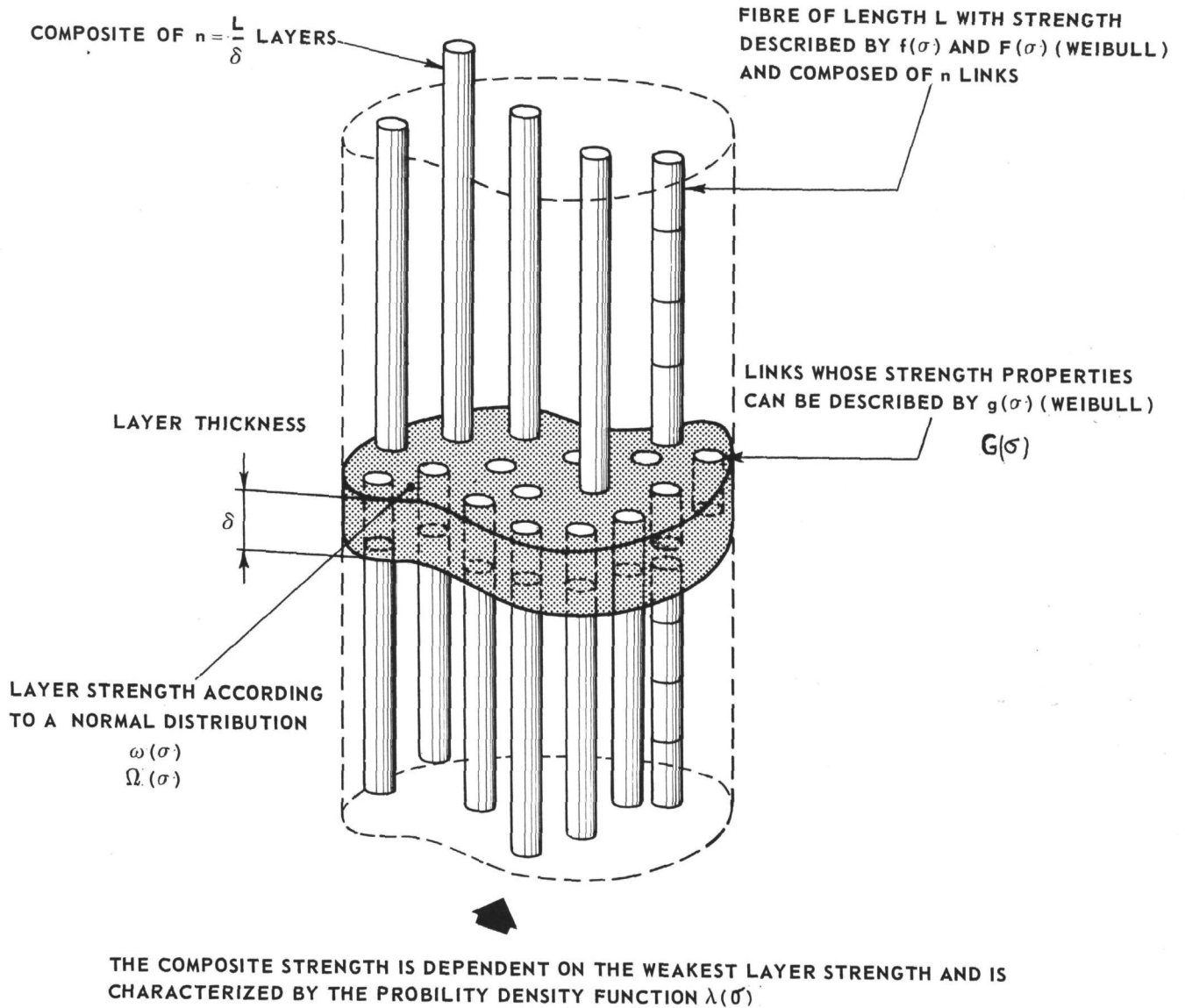


FIGURE 7 Three dimensional model of the cumulative weakening failure mode

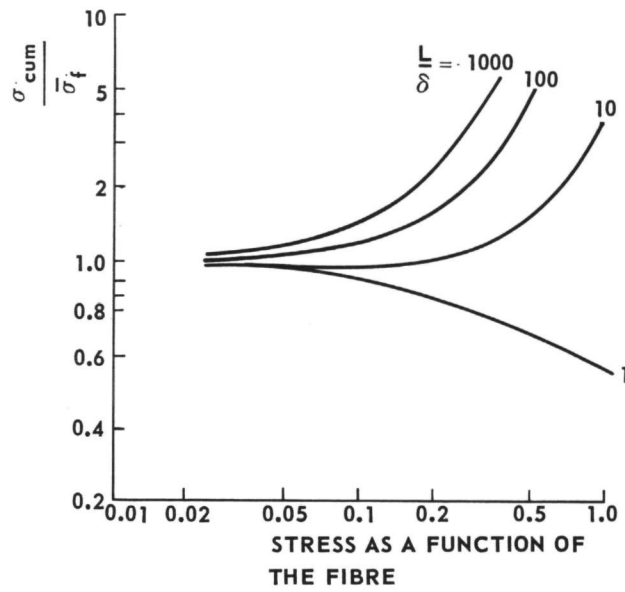


FIGURE 8 Normalized cumulative weakening stress as a function of the fibre coefficient of variation

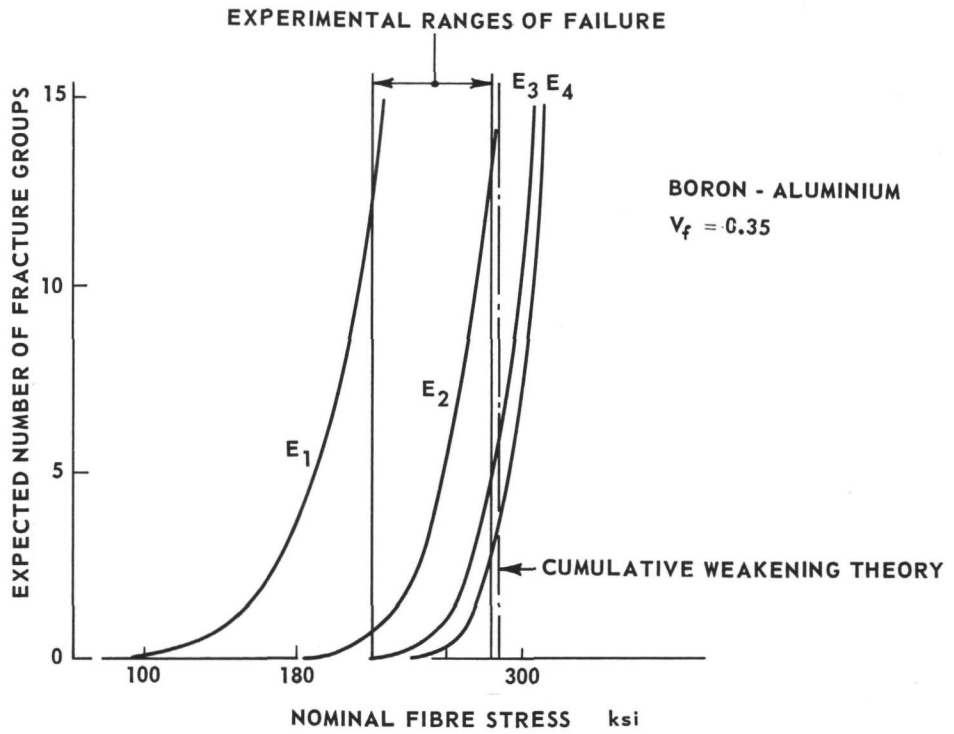


FIGURE 9 Expected number of fracture groups as a function of fibre stress (Ref. 12)

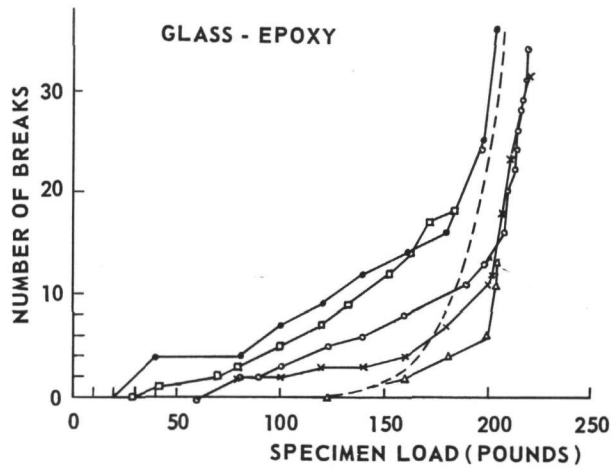
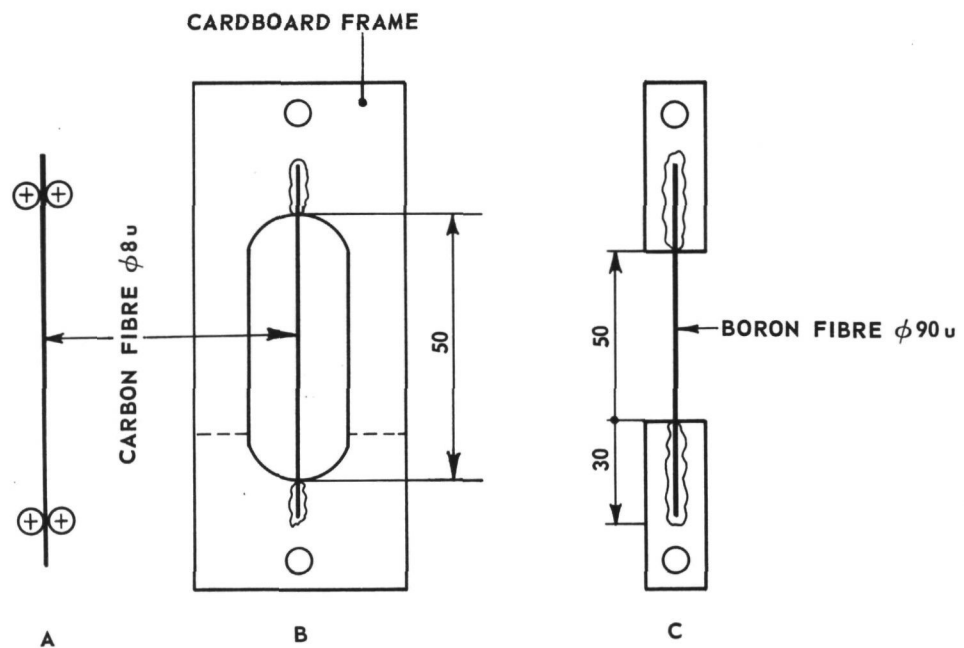


FIGURE 10 Number of fibre breaks as a function of applied load for five glass/epoxy specimens (Ref. 13)



**FIGURE 11** Methods of mounting carbon and boron fibres for single fibre testing

a: grips in the fafegraph testing machine

b: loading frame for carbon fibres

c: aluminium sheets of thickness .5 mm on which the boron fibre is mounted

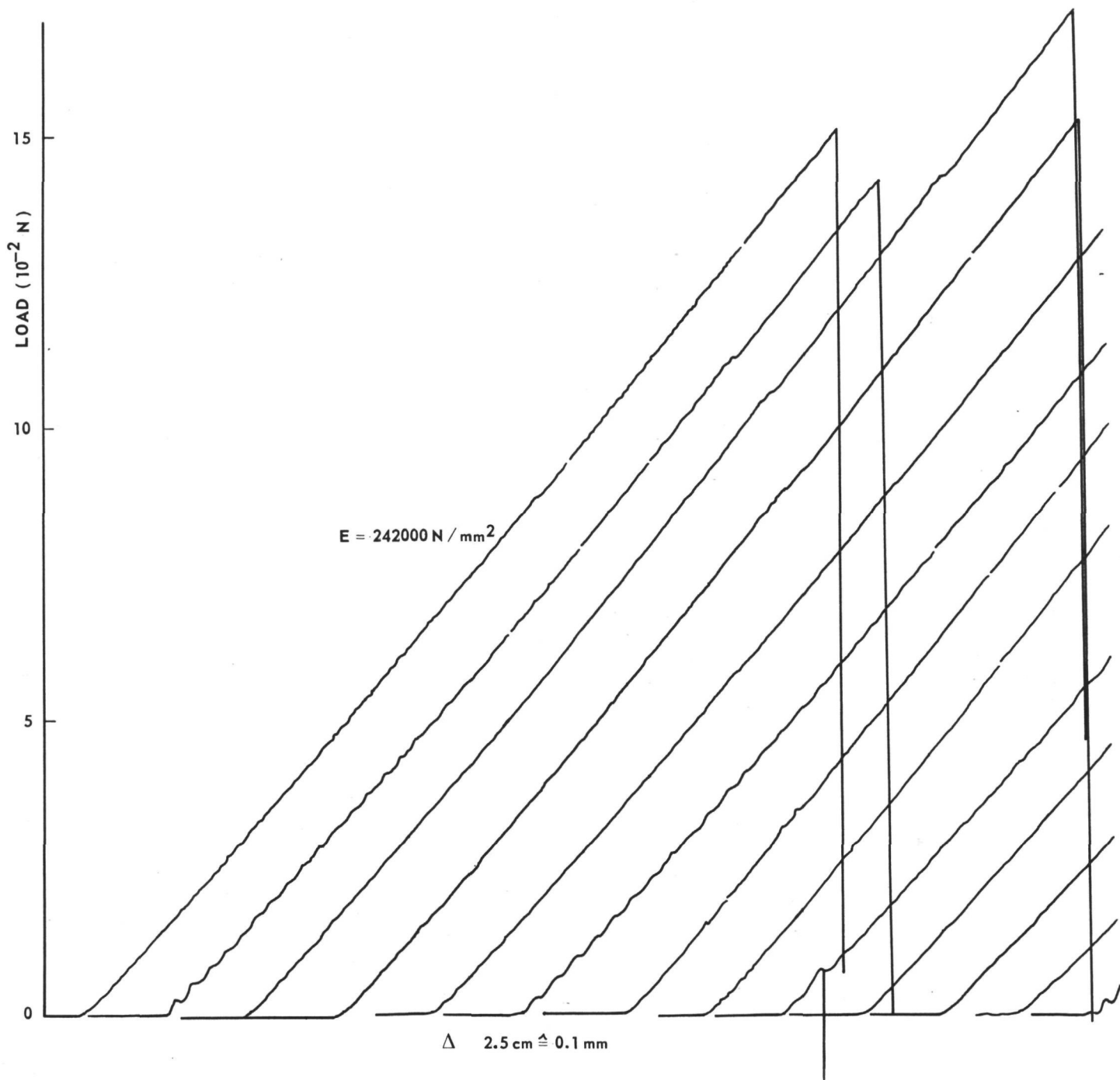


FIGURE 12 Load-displacement curves for carbon fibres

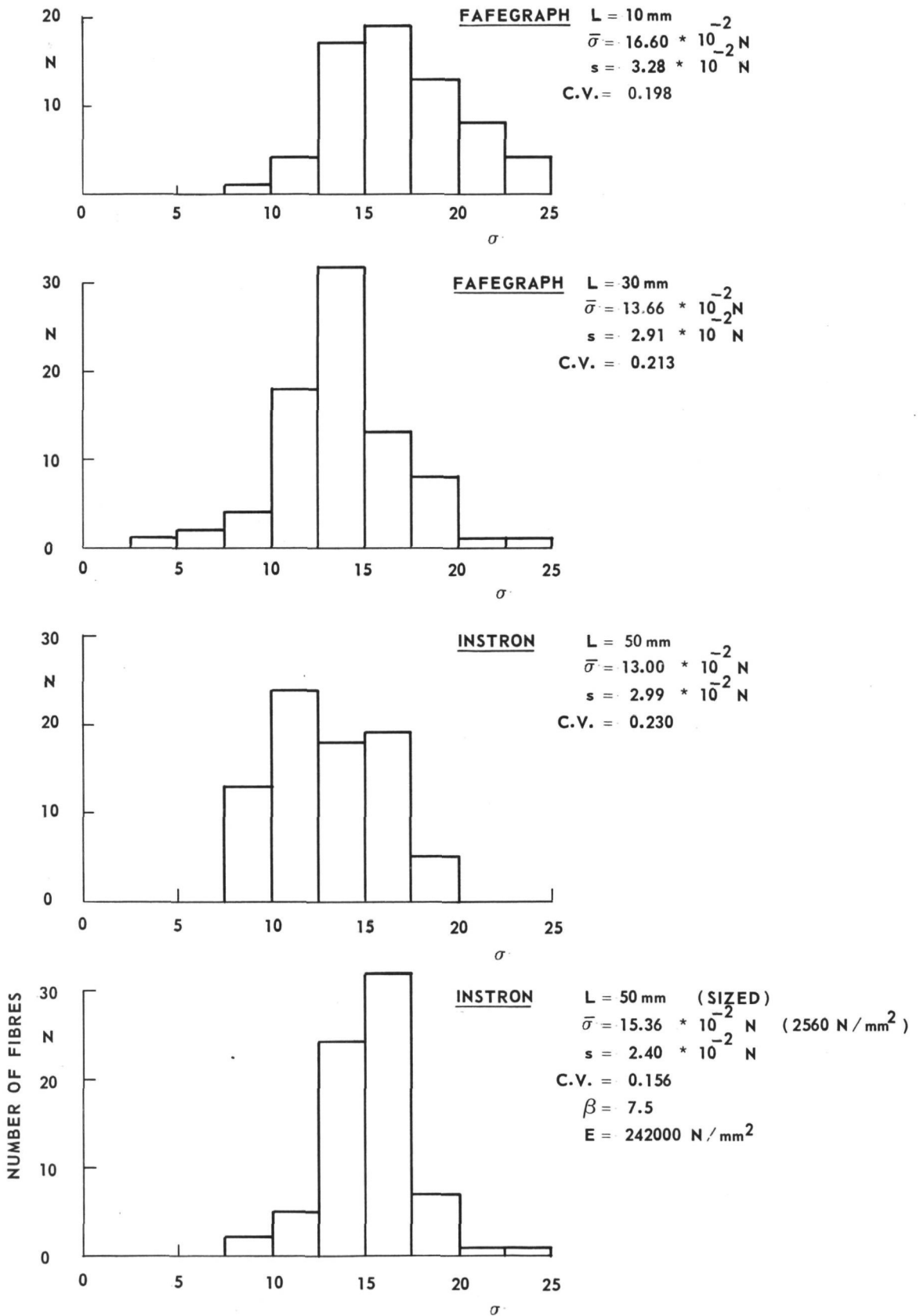


FIGURE 13 Histograms of the carbon fibre tests

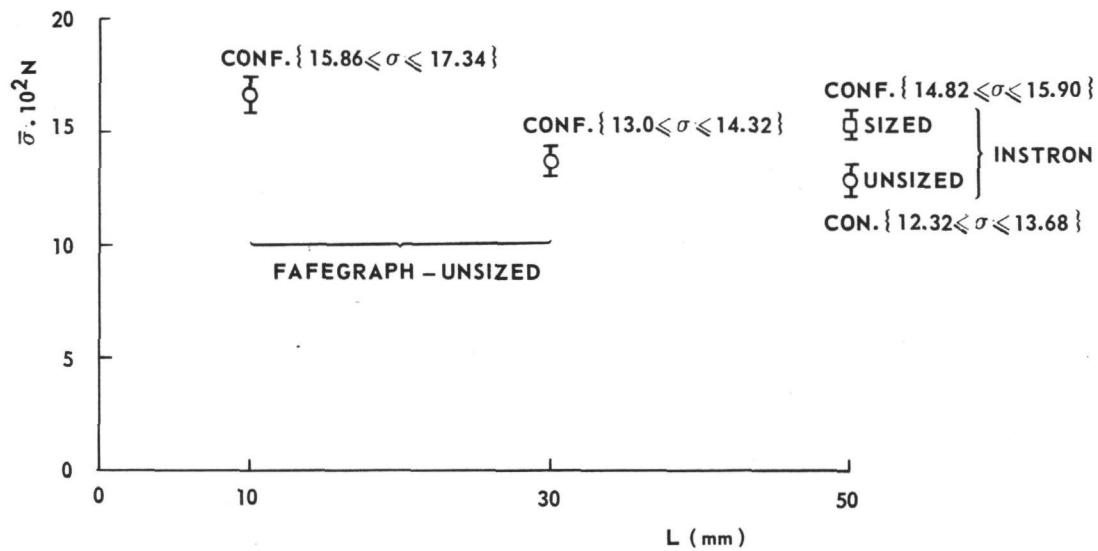


FIGURE 14 Length-strength dependence for carbon fibres

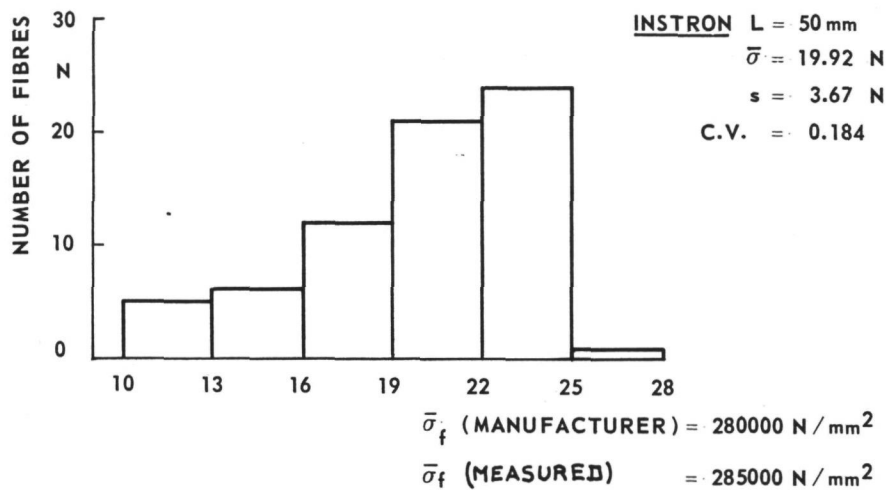


FIGURE 15 Histogram of the boron fibre tensile tests



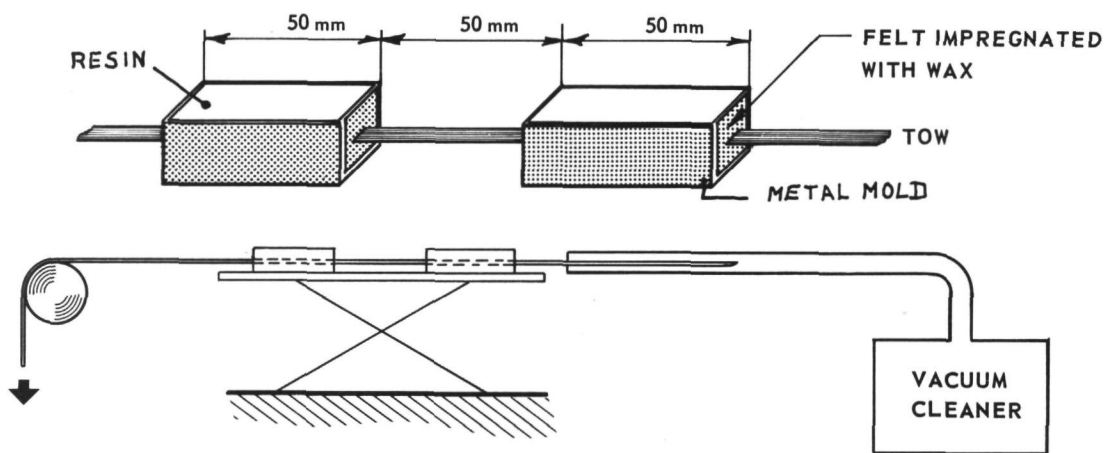
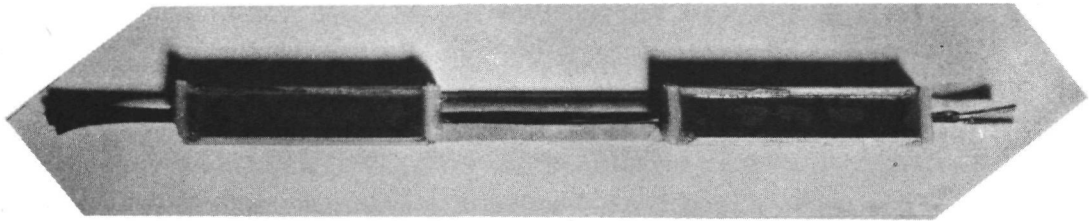
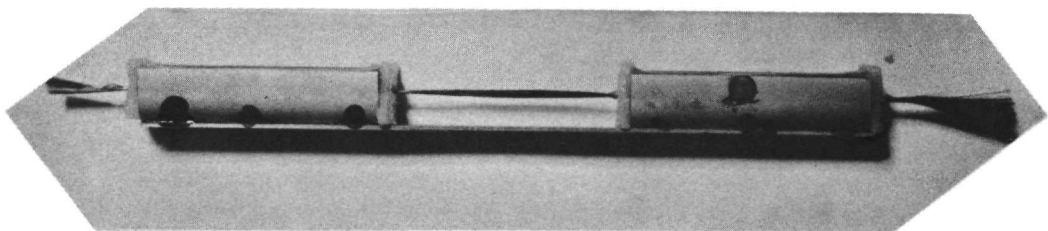


FIGURE 16 Preparation of bundle test specimen



TOP VIEW



FRONT VIEW

FIGURE 17 Bundle test specimens

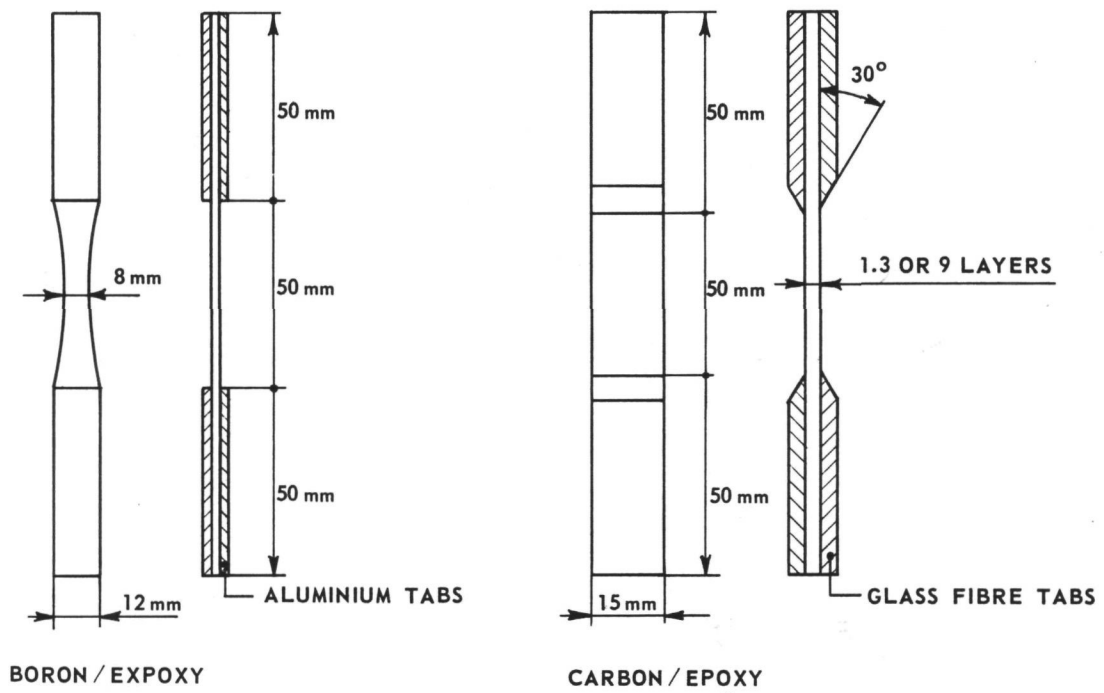


**FIGURE 18** Tensile specimens of unidirectional boron/epoxy and carbon/epoxy composites

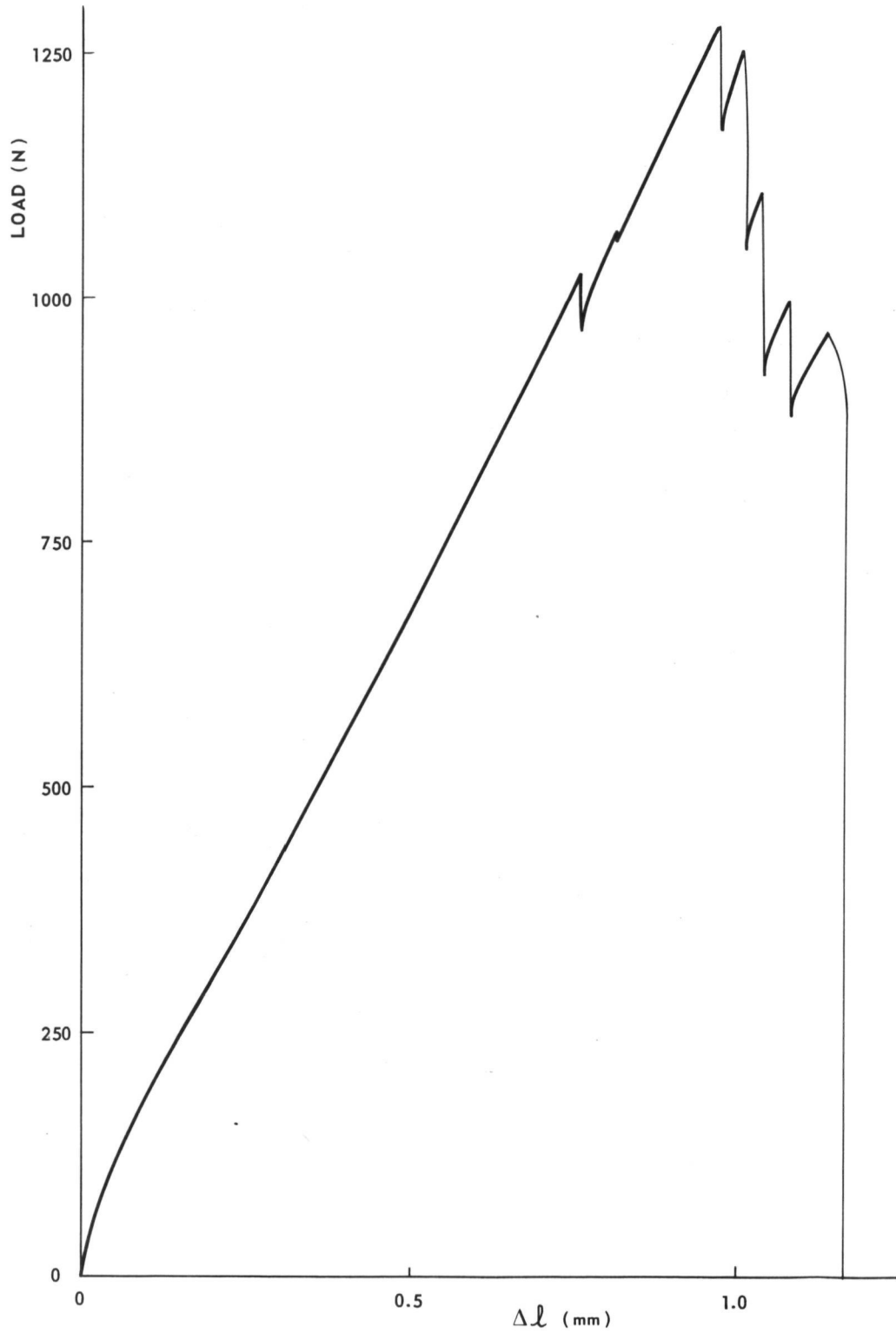
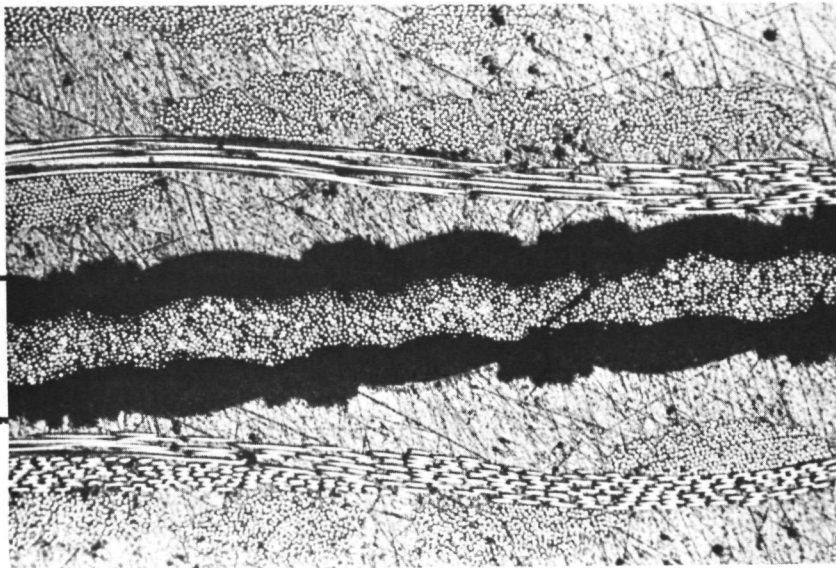
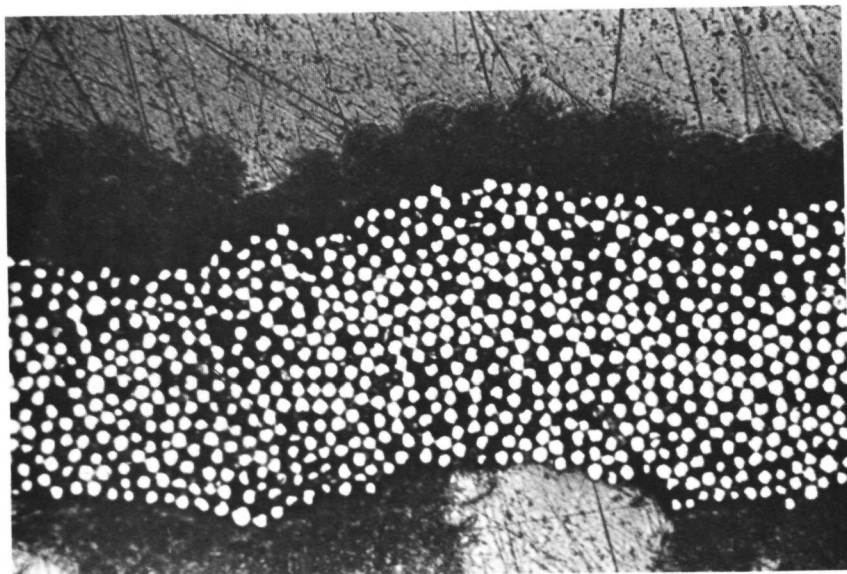


FIGURE 19 Load-displacement curve of a carbon/epoxy monopy specimen

FIBRE GLASS TABS.



72 X



288 X

NOTE CONSIDERABLE  
SCATTER IN FIBRE DIAMETER

FIGURE 20 Cross section of a carbon/epoxy monople

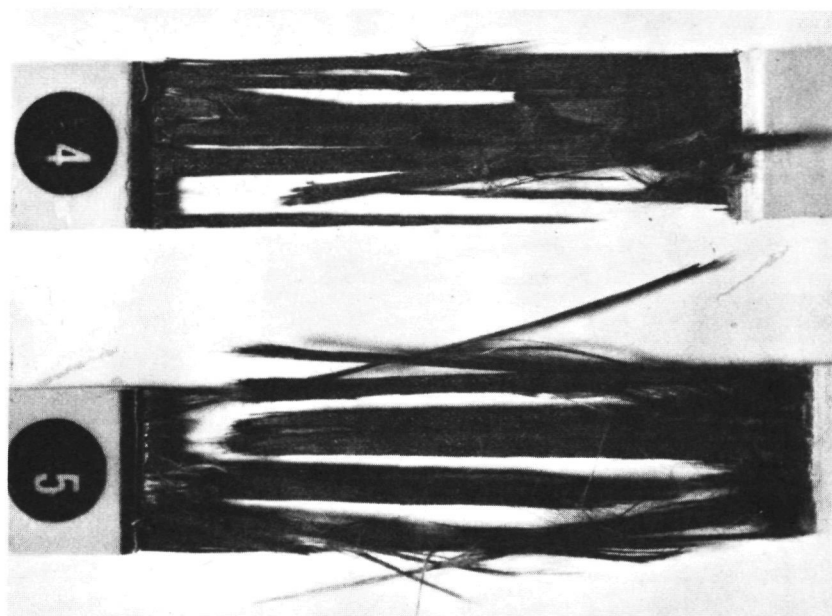
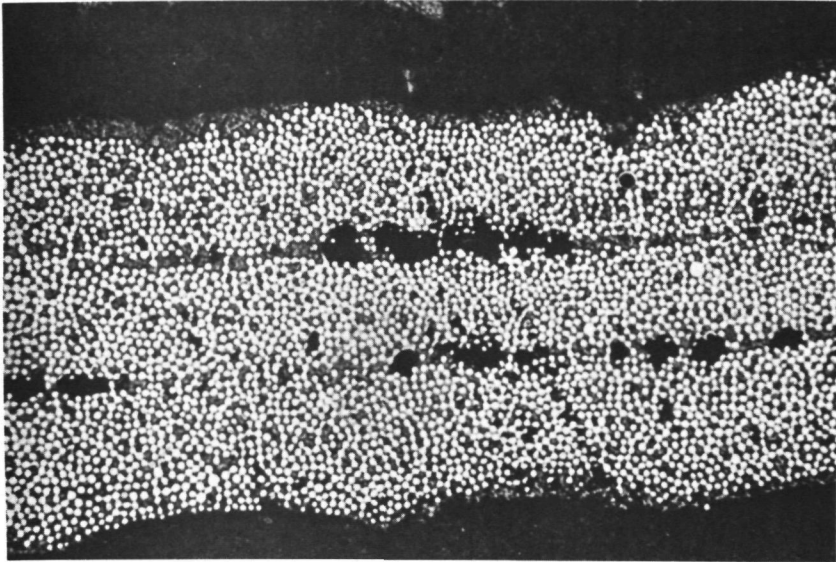
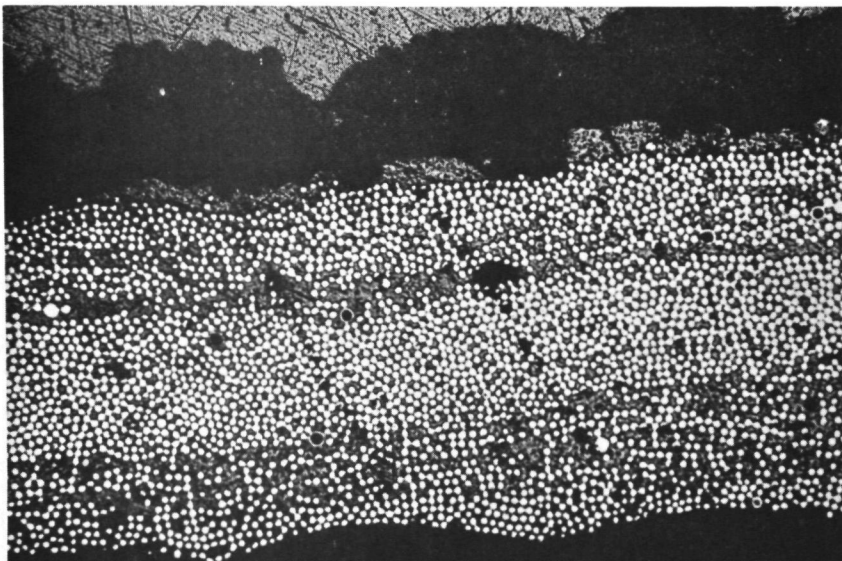


FIGURE 21 Splintered carbon/epoxy monopy specimens



144 X

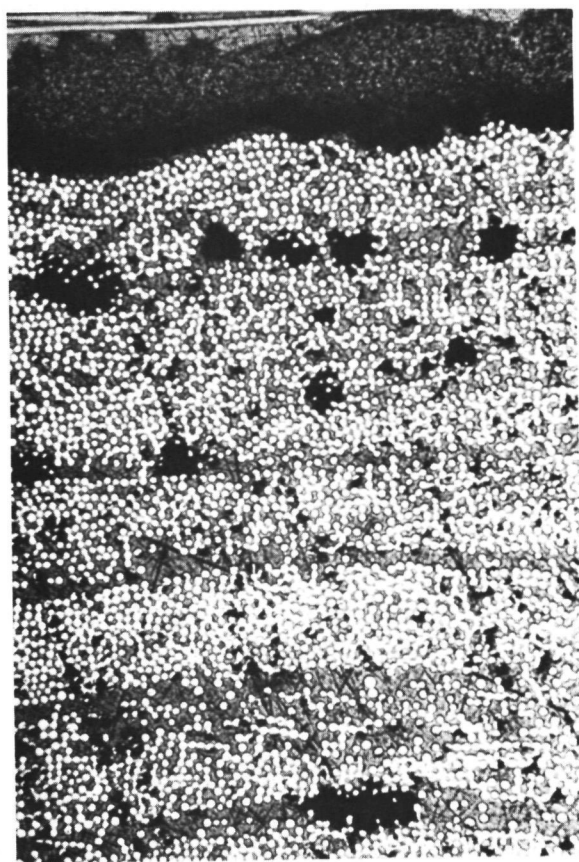
3-LAYER SPECIMEN



144 X

3-LAYER SPECIMEN

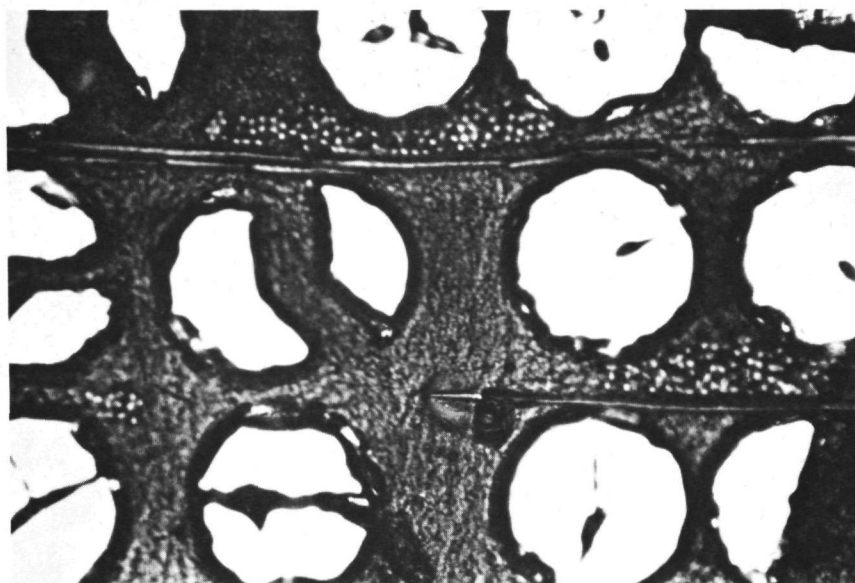
FIGURE 22 Cross section of a carbon/epoxy specimen showing voids and resin rich zones



144 X

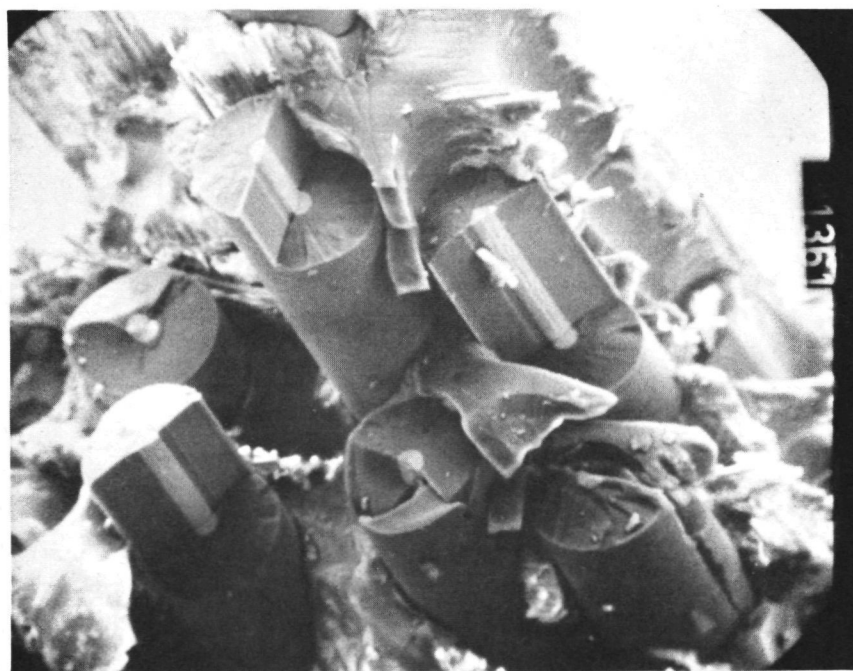
FIGURE 23 Carbon/epoxy specimen, showing a nonuniform fibre distribution





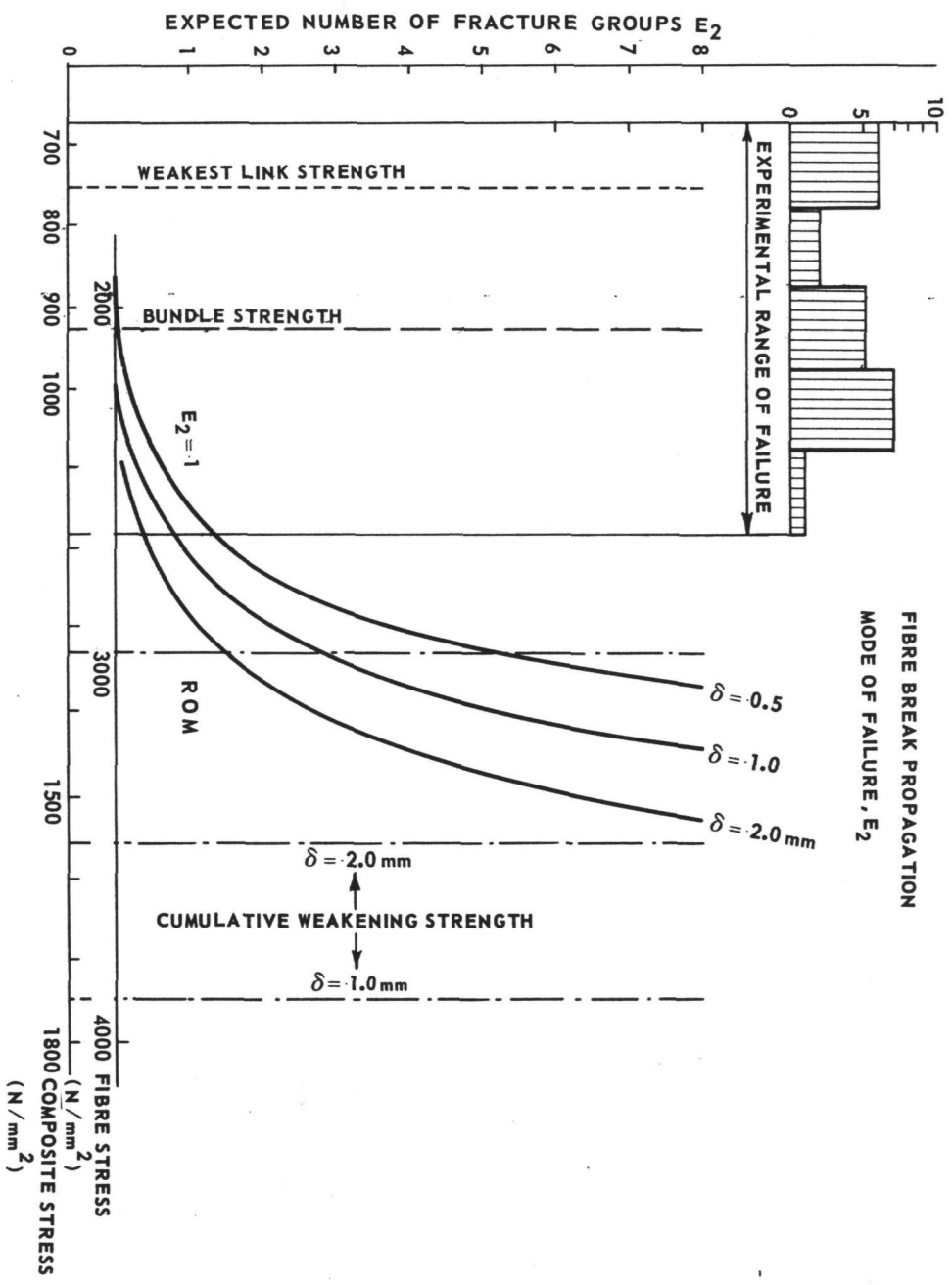
288 X

FIGURE 24 Split boron fibres in a composite cross section



120 X

FIGURE 25 Scanning electron microscope photograph of a boron/epoxy fracture surface



**FIGURE 26** Comparison of theoretical strength predictions and test results for boron/epoxy composites

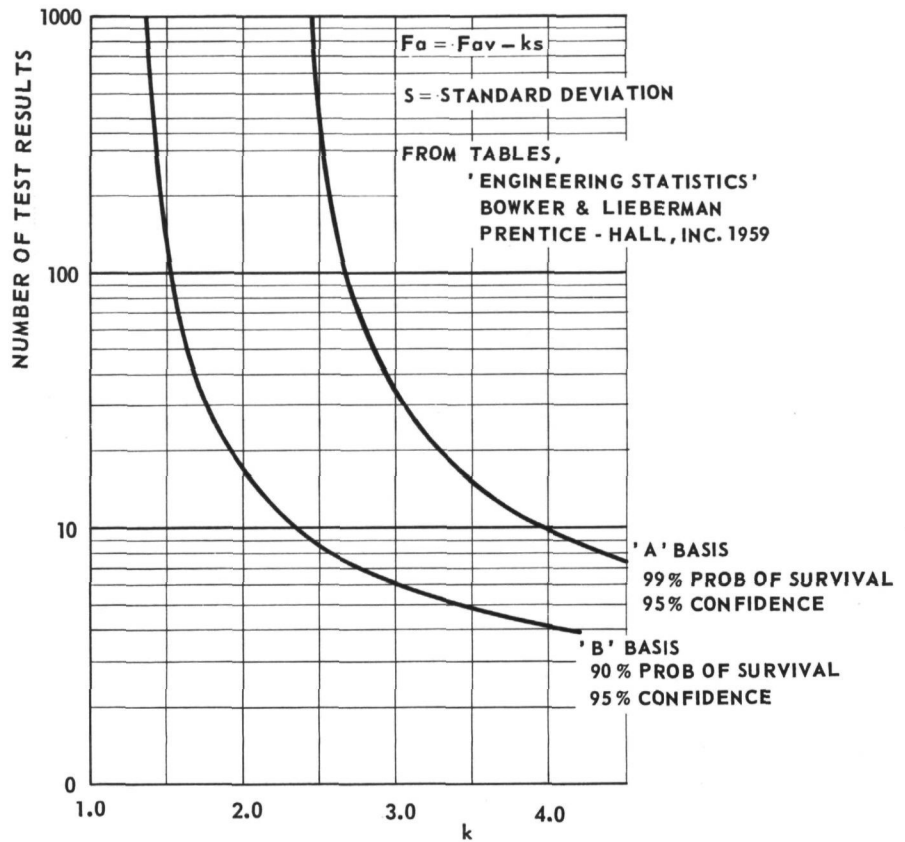


FIGURE 27 One-sided tolerance factors for normal distributions (Ref. 22)

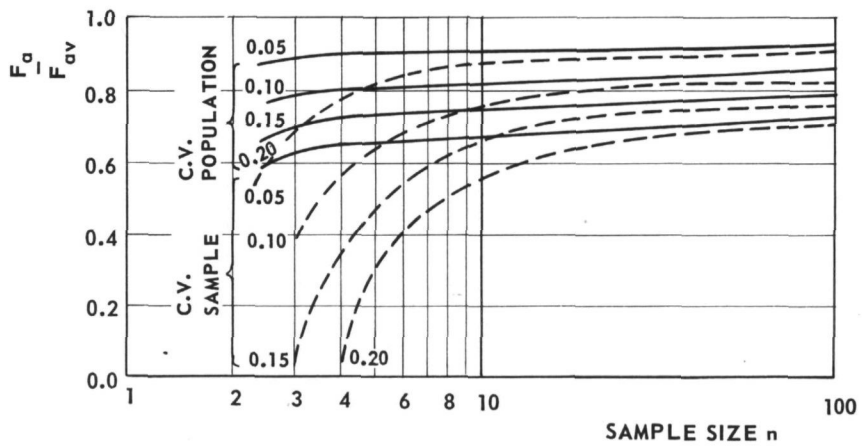


FIGURE 28 Design allowables based on population and sample coefficients of variation (Ref. 21)

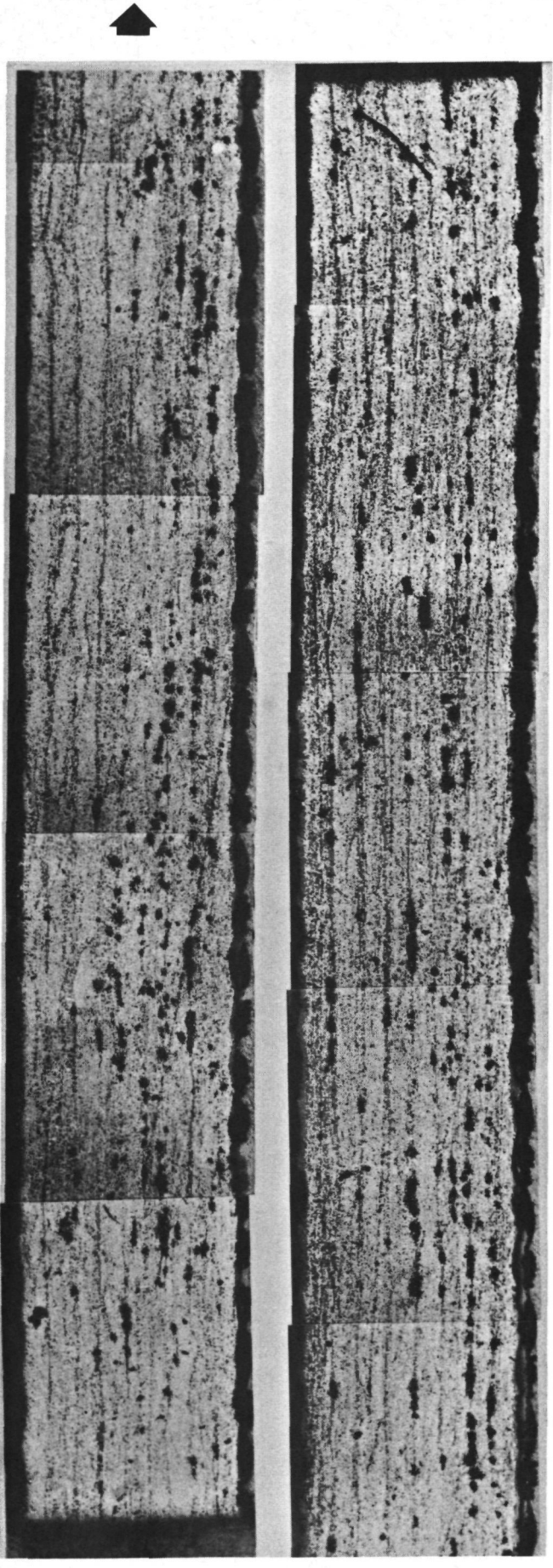
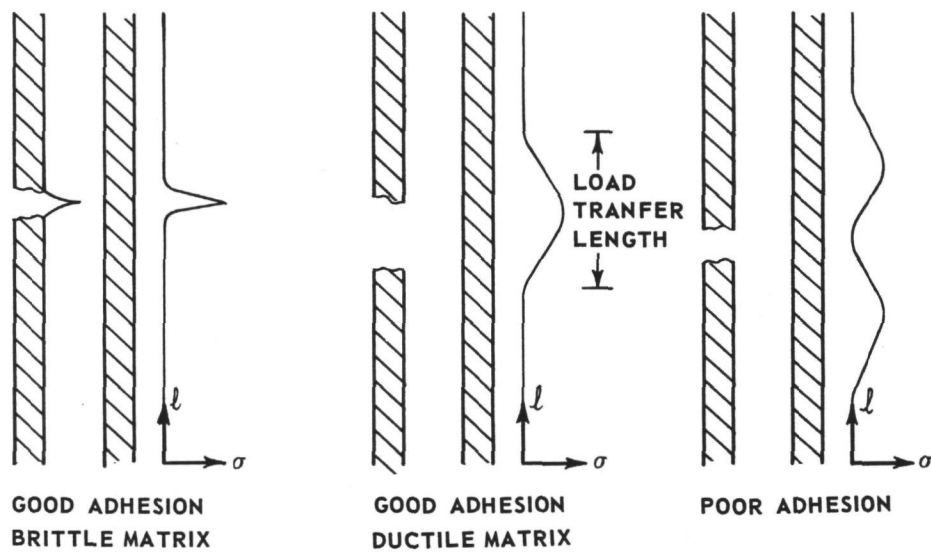


FIGURE 29 Cross section of a 9-layer carbon epoxy specimen (15 mm x 1 mm)



**FIGURE 30** Additional load enhancement in a fibre adjacent to a broken fibre dependent on the matrix and interface properties

